JBC Papers in Press. Published on December 29, 2016 as Manuscript M116.747766
The latest version is at http://www.jbc.org/cgi/doi/10.1074/jbc.M116.747766

A Quininib Analogue and Cysteinyl Leukotreine Receptor Antagonist Inhibits VEGF-Independent Angiogenesis and Exerts an Additive Anti-angiogenic Response with Bevacizumab

Clare T. Butler[1], Alison L. Reynolds[1], Miriam Tosetto[2], Eugene T. Dillon[1], Patrick Guiry[3], Gerard Cagney[1], Jacintha O'Sullivan[4], Breandán N.Kennedy[1#].

[1]UCD School of Biomolecular & Biomedical Science, UCD Conway Institute, University College Dublin, Belfield, Dublin 4, Ireland.

[2]Centre for Colorectal Disease, St Vincent's University Hospital, Dublin 4, Ireland.

[3]UCD School of Chemistry and Chemical Biology, UCD Centre for Synthesis and Chemical Biology, University College Dublin, Belfield, Dublin 4, Ireland

[4]Trinity Translational Medicine Institute, Department of Surgery, Trinity College Dublin, St. James's Hospital, Dublin 8, Ireland.

Running title: A *quininib analogue exhibits additive anti-angiogenic effects with bevacizumab*.

To whom correspondence should be addressed: Breandán N. Kennedy, F062 UCD Conway Institute, UCD School of Biomolecular & Biomedical Science, UCD Conway Institute, University College Dublin, Belfield, Dublin D04 V1W8, Ireland. Tel: +353 1 716 6740, email: brendan.kennedy@ucd.ie

Keywords: Drug development, angiogenesis, endothelial cell, migration, tubule formation, G-protein coupled receptor (GPCR), leukotriene, vascular endothelial growth factor (VEGF), colorectal cancer, calpain-2.

ABSTRACT

Excess blood vessel growth contributes to the pathology of metastatic cancers and age-related retinopathies (1). Despite development of improved treatments, these conditions are associated with high economic costs and drug resistance (2). Bevacizumab (Avastin®), a monoclonal antibody against vascular endothelial growth factor (VEGF) is used clinically to treat certain types of metastatic cancers (3,4). Unfortunately, many patients do not respond or inevitably become resistant to bevacizumab (5), highlighting the need for more effective anti-angiogenic drugs with novel mechanisms of action (6). Previous studies discovered quininib, an anti-angiogenic small molecule antagonist of cysteinyl leukotriene receptor 1 and 2 ($CysLT_{1\text{-}2}$) (7-9). Here, we screened a series of quininib analogues and identified a more potent anti-angiogenic novel chemical entity (IUPAC name: (E)-2-(2-quinolin-2-yl-vinyl)-benzene-1,4-diol-HCl) hereafter designated Q8. Q8 inhibits developmental angiogenesis in Tg(*fli1:EGFP*) zebrafish and inhibits human microvascular endothelial cell (HMEC-1) proliferation, tubule formation and migration. Q8 elicits anti-angiogenic effects in a VEGF-independent *in vitro* model of angiogenesis and exerts an additive anti-angiogenic response with the anti-VEGF biological bevacizumab. Cell-based receptor binding assays confirm Q8 is a $CysLT_1$ antagonist and is sufficient to reduce cellular levels of NF-kB and calpain 2 and secreted levels of pro-angiogenic proteins, ICAM-1, VCAM-1 and VEGF. Distinct reductions of VEGF by bevacizumab explains the additive anti-angiogenic effects observed in combination with Q8. In summary, Q8 is a more effective anti-angiogenic drug compared to quininib. The VEGF-independent activity coupled with the additive anti-angiogenic response observed in combination with bevacizumab demonstrates that Q8 offers an alternative therapeutic strategy to combat resistance associated with conventional anti-VEGF therapies.

INTRODUCTION

Angiogenesis is a highly regulated physiological process in health and disease which

enables the formation of new blood vessels (10). Enhanced angiogenesis occurs pathologically in response to hypoxia and inflammation in disorders such as cancer, psoriasis, blindness, diabetes and arthritis (11) impacting on the health of millions of people worldwide (2,11-13).

Angiogenesis is regulated by a balance of pro- and anti-angiogenic factors and arises from a stepwise process wherein endothelial cells dissociate from pericyte cells and their basement membrane moving towards the target tissue requiring vascularisation (14,15). Secreted factors can enhance or inhibit this process. Inducers of this process include vascular endothelial growth factors (VEGFs), angiopoietins, transforming growth factors (TGFs), platelet derived growth factors (PFGF), tumour necrosis factor-α (TNF-α), interleukins and fibroblast growth factor (FGF) proteins (16). Angiogenesis is also regulated by membrane bound proteins, including vascular cell adhesion protein-1 (VCAM-1) and intercellular adhesion molecule-1 (ICAM-1) which enable cell-matrix or cell-cell interactions (17-19). Angiogenesis is a frequently targeted process in the discovery of new drugs for cancer and blindness. Annual costs of cancer treatment and care are estimated to escalate to $173,000,000 in 2020 and the majority of new therapies cost ~$5,000 per month (20,21). Unfortunately, these expensive therapies often exert limited overall therapeutic benefit (22).

Bevacizumab (Avastin®), a monoclonal antibody against soluble VEGF, restricts the progression of tumor angiogenesis (23) and choroidal neovascularization (24) by preventing VEGF from interacting with vascular endothelial growth factor receptor-2 (VEGR2). However, a combination of this anti-VEGF biologic in combination with chemotherapy has limited therapeutic effects, merely prolonging the survival of metastatic colorectal cancer patients by ~4.7 months (25), lung cancer patients by ~13 months (26) and increasing progression-free survival of breast cancer patients by ~2-25 months (27,28). The clinical efficacy of bevacizumab is only apparent in combination with chemotherapy as it can stabilise leaky tumour vessels, enhancing delivery of chemotherapy to the tumour.

There is an unmet clinical need for the development of more effective treatments which have the ability to inhibit alternative regulators of angiogenesis, overcoming treatment resistance to anti-angiogenic therapy. New drug discovery is impeded by the small number of novel and validated disease targets (29). Target-based drug discovery focuses on specific known protein targets and overlooks the possible importance of less well functionally understood proteins that may be involved in disease mechanism. Hence, phenotype-based drug screening is re-emerging as an effective means of moving beyond well understood targets to discover novel drug targets and understand the physiology and pathophysiology of disease (29).

Previous phenotype-based chemical screens discovered quininib, a small quinoline molecule with novel anti-angiogenic activity (7-9). Quininib antagonizes cysteinyl leukotriene receptors-1 and 2 ($CysLT_{1\text{-}2}$), does not target VEGF receptors and inhibits p-ERK, a $CysLT_1$ downstream effector (7). Cysteinyl leukotrienes, LTC_4, LTD_4 and LTE_4 are lipid mediators produced from arachidonic acid via the 5-lipoxygenase pathway (30). They are agonists for the G-protein coupled cysteinyl leukotreine receptors $CysLT_1$, $CysLT_2$ and the less functionally studied GPR17 and GPR99 ($CysLT_3$) (31).

CysLT receptors are abberantly expressed in tumours; enhanced expression of $CysLT_1$ in colorectal cancer negatively correlates with patient survival (32) and antagonism of $CysLT_1$ significantly reduces angiogenesis in rodent models (33). Collectively, this reveals an important biological role for cysLT signalling during neovascular disease and as an alternative therapeutic target.

Here, 24 structurally distinct analogues of quininib were ranked. Analogues Q22, Q18 and Q8 were significantly more effective than quininib at inhibiting angiogenesis *in vivo* with Q8 being the most potent analogue. Q8 inhibits human endothelial cell tubule formation and migration. Ligand binding assays confirm that Q8 is also a $CysLT_1$ antagonist. Further to what we previously reported regarding the mechanism of action of quininib (7), the structurally distinct Q8 analogue significantly reduces cellular levels of pro-angiogeneic signals NF-kB and calpain-2 and secreted levels of ICAM-1, VCAM-1 and VEGF compared to quininib. Additionally, Q8 inhibits *in vitro* models of angiogenesis which do not rely on endogenous VEGF and exerts an additive anti-angiogenic effect with bevacizumab.

RESULTS

Analogues have enhanced anti-angiogenic effects in vivo compared to Q1. The small molecule quininib (Q1) was previously identified to inhibit ocular angiogenesis in the zebrafish hyaloid vascular assay and tumour angiogenesis (7-9). Here, we sought to identify novel chemical entities with more potent anti-angiogenic effects *in vivo* using the zebrafish intersemental vessel assay. Preliminary analyses of 37 structural quininib analogues identified drugs that robustly inhibited developmental angiogenesis in larval zebrafish eyes (34). In these analogues, the position of the phenyl ring hydroxy group and/or the linkage between the quinoline and phenyl ring was modified (**Fig. 1A**). Initially, we ranked the bioactivity of 24 salt or amine analogue formulations by comparing the ability of 10 µM of the drugs to inhibit developmental angiogenesis in the intersegmental vessel (ISV) assay using Tg[*fli1*:EGFP] zebrafish (**Fig. 1B, 1C**). Twelve analogue formulations produced a statistically significant inhibition of developmental angiogenesis compared to control (**Fig. 1C**). Of these, one analogue Q22 produced anti-angiogenic activity equivalent to quininib, and two analogues Q22 and Q18 produced a greater anti-angiogenic activity compared to quininib at 10 µM ($p<0.05$) (**Fig. 1C**). Q22 (IUPAC name: 2-quinolin-2-yl-ylethynyl-phenol) includes an alkyne linkage between the quinoline and phenyl ring whereas Q18 (IUPAC name: (*Z*)-2-(2-(quinolin-2-yl)vinyl) phenol HCl) is the Z-enantiomer of quininib. Notably, Q7 in amine and hydrochloride salt forms was toxic to larvae at 10 µM. Q7 (IUPAC name: (*E*)-2-(2-quinolin-2-yl-vinyl)-benzene-1,4-diol) includes two hydroxy groups in the phenyl ring at positions R_1 and R_4. Quininib, Q18, Q22 and Q8 were re-screened in the ISV assay at concentrations increasing from 0.1-10 µM (**Fig. 1D-E**). All novel analogues tested resulted in a dose-dependent inhibition of ISV development. Interestingly, only Q8 and Q18 were significantly bioactive at 1 µM, reducing ISV development compared to control, by 75% and 30%, respectively (**Fig. 1E**). Q8 reduced ISV development more potently than any other analogue tested and was the only analogue significantly active at 0.5 µM inhibiting developmental angiogenesis by 12.4%. All analogues produced varying degrees of pericardial oedema at 2 dpf. No other adverse morphological defects were detected following treatment with the analogues at 2 dpf (**Fig 1. D**). In summary, using an analogue ranking system based on maximum inhibition of ISV and potency, Q8 was identified as the most effective quininib analogue **(Table 1.**

Quininib analogues reduce endothelial cell number after 24 hours and inhibit endothelial cell migration. Quininib and the highest ranking analogues were tested for effects on HMEC-1 endothelial cell number following 24, 72 and 96 hours treatment (**Fig. 2A**). 10 µM quininib and analogues had no effect on HMEC-1 cell number compared to control at 24 hours. However, at 72 hours, 5-Fluorouracil (5-FU), Q8 and Q18 significantly reduced endothelial cell number compared to vehicle controls ($p>0.001$). At 96 hours treatment, all compounds reduced cell number significantly compared to 0.1% DMSO controls.

Using a CIM-plate 16 xCELLigence® RTCA platform, the migratory behaviour of drug treated HMEC-1 endothelial cells was quantified over 8 hours (**Fig. 2A**). All analogues except quininib (Q1) significantly inhibited HMEC-1 endothelial cell migration with Q8 producing the most significant effect, inhibiting endothelial migration by ~79% ($p<0.001$). (**Fig. 2B**). We also investigated if a combination of either 1 or 3 µM Q8 with bevacizumab had additive effects on HMEC-1 endothelial cell migration (**Fig. 2C**). Compared to control, 2.5 µg/µl bevacizumab, 1 µM or 3 µM Q8, or 2.5 µg/µl bevacizumab in combination with 1 µM Q8 treatments did not significantly reduce HMEC-1 migration. However, 2.5 µg/µl bevacizumab in combination with 3 µM Q8 significantly reduced migration compared to control ($p<0.046$) and to 2.5 µg/µl bevacizumab ($p<0.039$) but not to 3 µM Q8 alone ($p<0.2615$). As observed with previous migration analyses, 10 µM Q8 induced the most statistically significant reduction of HMEC-1 cell migration compared to control ($p<0.002$).

In summary, Q8 and Q18 significantly reduced HMEC-1 endothelial cell number at 72 and 96 hours, whereas quininib (Q1) and Q22 showed significant reductions in cell number at 96 hours only. Analogues of quininib, particularly Q8, impede endothelial cell migration, a surrogate measure of angiogenesis.

Quininib analogues inhibit human endothelial cell tubule formation and do not affect

HMEC-1 viability. Previous studies demonstrated that 10 μM quininib (Q1) had modest effects on endothelial tubule formation in human dermal microvascular endothelial cells (HMVECs) (35). Here, we tested the dose-dependent effects of quininib (Q1) and its analogues (Q8, Q18, Q22) on HMEC-1 tubule formations using μ-slide angiogenesis plates (IBIDI). Quininib (Q1) significantly inhibited tubule formation at 3 and 10 μM, but not at 1 μM (**Fig 3. A**). Following 16 hours treatment, Q8 and Q18 were significantly more effective than quininib at inhibiting HMEC-1 tubule formation at all concentrations tested (1-10 μM) (p<0.01). Q8 and Q18 were the most effective compounds, inhibiting tubule formation at 10 μM by ~98% and 78%, respectively (p<0.05). Potential cytotoxic effects of analogue Q8 were ruled out by co-staining HMEC-1 endothelial cell tubules with calcein and propidium iodide (PI) following 16 hour exposure (**Fig 3. C**). No concentrations of Q8 tested (0.01 – 20 μM) induced any significant endothelial cell death as shown by a lack of PI staining (red) compared to cells treated with 10 μM sunitinib which stained positively for PI (**Fig 3. C**). In addition, calcein was taken up by the cells treated with all concentrations of Q8 (green) indicating that HMEC-1 cells are viable following 16 hour treatment with the Q8 analogue.

Quininib analogues inhibit VEGF-independent angiogenesis in vitro. We investigated the effects of the clinically used VEGF neutralizing antibody bevacizumab on tubule formation by incubating HMEC-1 cells with varying concentrations of bevacizumab ranging from (2.5-10 μg/μl), all of which had no effect on tubule formation compared to control or IgG isotype control (**Fig 4. A, B**). Furthermore, higher concentrations of bevacizumab (5 and 10 μg/μl) did not significantly affect HMEC-1 tubule formation (data not shown). The addition of 10 ng/ml recombinant VEGF increased endothelial cell tubule formation by ~20% compared to control (p=0.0082). Following addition of both 2.5 μg/μl bevacizumab and 10 ng/ml VEGF, tubule formation was significantly decreased by ~45% compared to 10 ng/ml VEGF alone (p<0.05) (**Fig 4. A, B**). We conclude that our HMEC-1 *in vitro* tubule formation assays are not dependent on basal VEGF but exogenous VEGF is sufficient to induce enhanced tubule formation. We examined the effects on tubule formation when treating cells with quininib or Q8 in the presence of exogenous VEGF-induction. Interestingly, ectopic VEGF could suppress the anti-angiogenic effects of quininib drugs but not the anti-VEGF biological, supporting distinct mechanisms of action of these anti-angiogenic drugs. In the presence of exogenous VEGF, quininib or Q8 produced a more modest inhibition of tubule formation compared to treatment with either alone (**Fig 4. C, D**). In summary, the quininib small molecule drugs are efficacious at inhibiting a VEGF-independent model of *in vitro* angiogenesis. The VEGF-independent anti-angiogenic action of these drugs is further supported by a lowered anti-angiogenic activity in the presence of recombinant VEGF.

Q8 has additive anti-angiogenic effects with an anti-VEGF biologic, bevacizumab. The distinct mechanisms of actions inferred above led us to investigate the *in vitro* anti-angiogenic effects of our lead small molecule drug Q8 in combination with bevacizumab. HMEC-1 endothelial cells were treated with a combination of either 3 μM Q1 and 2.5 μg/μl bevacizumab or 1 μM Q8 and 2.5 μg/μl bevacizumab (**Fig. 5 A, B**). Concentrations of Q1 (3 μM) and Q8 (1 μM) producing equivalent (p=0.1163) (~45-65%) intermediate responses were selected for the combination study (**Fig 3. A**). As bevacizumab requires the presence of exogenous VEGF to bring about an anti-angiogenic effect (**Fig 4. A)**, combination treatment groups were supplemented with 10 ng/ml recombinant VEGF. Compared to either Q8 or bevacizumab treatment alone, treatment of HMEC-1 cells with the combination of Q8 and bevacizumab induced an additive significant reduction in tubule formation (p=0.0174) (**Fig 5. A, B**). This additive effect was observed with Q8 and not with quininib (Q1) (**Fig 5. A, B**). There was no statistically significant difference in tubule formation observed between Q8 alone and bevacizumab alone treatment groups. In addition, an isotype control which consisted of a combination of 1 μM Q8 and 2.5 μg/μl IgG did not alter tubule formation compared to Q8 or bevacizumab alone. However, compared to the isotype control combination treatment, 1 μM Q8 and 2.5 μg/μl bevacizumab combination treatment significantly reduced tubule formation, signifying the specificity of bevacizumab in the anti-angiogenic combination effect. In conclusion, specific, enhanced anti-angiogenic effects are demonstrated following treatment of human

endothelial cells with a combination of both Q8 and an anti-VEGF biologic, bevacizumab.

*Quininib analogue Q8 is a cysteinyl leukotriene receptor-1 antagonist and regulates inflammatory and angiogenic signalling pathways***.** The $CysLT_1$ receptor was previously identified as a quininib target (7). Here, we determined the IC_{50} of Q8 for $CysLT_1$ receptor to be 4.9 µM in a CHO cell-based receptor antagonism assay. The highest concentration of Q8 tested (50 µM) inhibited $CysLT_1$ activation by 113% (**Fig 6. A**). In contrast, Q8 produced only a 22.9% antagonism of $CysLT_2$ receptor activation in HEK-293 cells. Thus, Q8 was excluded as a $CysLT_2$ antagonist as inhibition lower than 50% is considered insigificant. In relation to VEGF receptors, above threshold inhibiton was only observed with VEGF2 or VEGF3 at higher concentrations. Using a cell-based ligand binding assay, 10 µM Q8 only inhibited [^{125}I]VEGF binding to VEGFR1 by 23%, well below the 50% inhibition cut-off regarded as significant (http://www.eurofins.com/biopharma-services/discovery/). Similarily, 1 or 3 µM Q8 did not inhibit the kinase activity of VEGFR2, or VEGFR3 producing inhibitions (-34 to -24% or 29 to 46%, respectively) below the 50% threshold. However, 10 µM Q8 inhibited VEGFR2 kinase activity by 65% and VEGFR3 kinase activity by 78%.

We correlated the expression levels of $CysLT_1$ in Tg[*fli1*:EGFP] zebrafish larvae and in HMEC-1 endothelial cells during time-points when quininib analogues induced anti-angiogenic phenotypes (**Fig 6. B**). Levels of $CysLT_1$ gene expression were highest in 2 dpf Tg[*fli1*:EGFP] larvae (stage of intersegmental vessel growth analyses) compared to 6 hpf and 3 dpf larvae (**Fig 6. B**) The $CysLT_1$ receptor is traditionally associated with a cell membrane location, however, $CysLT_1$ also resides within the nuclear compartment (32). We demonstrate that the nuclear form of $CysLT_1$ is abundantly expressed in the HMEC-1 cells utilised for tubule formation and migration assays (**Fig 6. B**). We treated HMEC-1 endothelial cells for 5 hours with 10 µM Q1, Q8 and the clinically used bronchodilator and anti-inflammatory $CysLT_1$ antagonist, montelukast. Q8 reduced expression levels of the putative downstream $CysLT_1$ mediator calpain-2 by ~22% compared to control (p=0.0425) but there was no significant change in levels of calpain-2 following treatment of HMEC-1 cells with Q1 or montelukast (**Fig 6. C**). Furthermore, we analysed activated NF-kB p65 in HMEC-1 cell lysates and found 10 µM Q8 reduced NF-kB levels by ~32% (p<0.001) compared to control. In contrast, there were no significant changes in activated levels of NF-kB p65 following treatment with Q1 or montelukast (**Fig 6. D**). To determine if levels of positive regulators of angiogenesis were altered by quininib analogues, secretions of Ang-1, Ang-2, bFGF, VEGF, ICAM-1 and VCAM-1 were quantified from HMEC-1 endothelial cells following treatment with 10 µM quininib, Q8, Q22, Q18 and 2.5 µg/µl bevacizumab (**Fig 6. E**). Ang-1 secretion was reduced by quininib, Q8 and Q18, but not by the anti-VEGF bevacizumab. VEGF levels were significantly decreased by Q8 and bevacizumab only. Ang-2 secretion was reduced by all compounds including bevacizumab. Q8 was the only drug which significantly reduced the secretions of soluble VCAM-1 and ICAM-1 (**Fig 6. E**). The dual attenuation by bevacizumab and Q8 on VEGF levels, together with the exclusive attenuation by Q8 on levels of ICAM-1 and VCAM-1 may explain the additive anti-angiogenic effect observed with bevacizumab and Q8 in combination

In summary, Q8 is a $CysLT_1$ antagonist with an IC_{50} of 4.9 µM. $CysLT_1$ is expressed in the zebrafish developmental stages and human endothelial cells in which quininib analogues exert anti-angiogenic effects. Q8 significantly reduces endothelial cell secretion of the pro-angiogenic $CysLT_1$ downstream mediators VEGF, ICAM-1, VCAM-1, NF-kB and calpain-2. Q8 can produce anti-angiogenic effects independent of VEGF, supporting a distinct mechanism of action. Q8 also exerts an additive anti-angiogenic response in combination with the anti-VEGF bevacizumab, likely due to some key pro-angiogenic factors being mutually reduced by both drug agents and others specifically reduced by bevacizumab or Q8.

DISCUSSION

Organ growth and reparation relies on the growth of additional vasculature through angiogenesis. However, a disparity in the regulation of this process leads to various pro-angiogenic diseases including cancer, blindness and rheumatism and it is estimated that ~500,000,000 people will benefit from the development of anti-

angiogenic therapies over the next 20-30 years (12).

The most recognized anti-angiogenic therapies are the anti-VEGFs, particularly the $VEGF_{165}$ recombinant humanized monoclonal antibody bevacizumab (Avastin®) (12). Despite the promising effects that bevacizumab exhibited in animal models of tumour growth, it only extends life in colorectal cancer patients by ~4.7 months (25), in non-small-cell lung cancer (NSCLC) by ~13 months (26), in cervical cancer by ~17 months (36) and it failed to show any overall survival benefit in breast cancer patients (28). Given the evolving evidence that mediators other than VEGF promote the angiogenic switch in malignancy (37), the clinical potential for combining an anti-VEGF biological with an inhibitor of a novel pro-angiogenic target is irrefutable (12). Such an approach could reduce clinical resistance to anti-angiogenic therapy and increase treatment efficacy (38).

Phenotype based screening of a library of small molecules led to the identification of the $CysLT_1$ antagonist quininib, a novel inhibitor of ocular and tumour angiogenesis (7,9). Through structural modification of quininib, analogues which more effectively and potently inhibit intersegmental vessel formation in zebrafish larvae were developed. Indeed, the anti-angiogenic effects of clinically tested agents such as SU5416 have been validated using zebrafish vasculature assays (39). Our highest ranking anti-angiogenic analogue from *in vivo* dose-dependent screening was Q8, also a $CysLT_1$ antagonist. Stimulation of $CysLT_1$ signaling by endogenous ligand LTD_4 leads to activation of downstream mediators phospholipase C (PLC), phosphoinositide 3-kinase (P13K) and protein kinase C-alpha (PKCα) (40). These mediators converge to promote angiogenic processes through activation of cell migration and motility, cell proliferation and survival and increasing levels of secreted VEGF through activation of NF-kB (**Fig 7. A**). Thus, antagonism of $CysLT_1$ can inhibit these pro-angiogenic processes. The parent compound, quininib (2-[(*E*)-2-(quinolin-2-yl)vinyl] phenol), was first chemically described as an antagonist of $CysLT_1$ by Zamboni *et al* (41). The positional substitution of quininib by way of inclusion of a hydroxy group in the R_1 position of the phenyl ring and incorporation of an (*E*)-ethenyl linkage between the quinoline and the phenyl ring gave rise to optimal $CysLT_1$ binding (41). The enhanced potency of Q8 compared to quininib and other analogues is likely due to the additional phenyl ring hydroxy group in the R_4 position. A structure-activity relationship study (42), highlighted the importance of hydroxy group positioning for the biological activity of the anti-estrogen drug tamoxifen, demonstrating that specific hydroxy positioning enabled correct configuration of the alkylaminoethane side chain of tamoxifen facilitating binding to the estrogen receptor. It is suggested that the carboxylate groups of the endogenous $CysLT_1$ ligand LTD_4 are recognized by the hydrophilic (ionic) binding site of $CysLT_1$ (41) and it is probable that the additional R_4 hydroxy group of the Q8 aryl ring leads to enhanced interaction with $CysLT_1$ through either additional hydrogen bonding or through the more electron-rich aryl system through π-π interactions.

Emerging evidence highlights the functional importance of the leukotrienes acting via $CysLT_1$ during blood vessel growth (7,43). LTC_4, LTD_4 and LTE_4 are lipids that induce inflammation by binding to and activating $CysLT_1$ and $CysLT_2$ and the less functionally studied GPR17 and GPR99 ($CysLT_3$) (31). Increased production of TNF-α and NF-kB following $CysLT_1$ activation leads to upregulation of VEGF and matrix metalloproteinases leading to enhanced endothelial cell proliferation, migration and vascular tubule formation (30). Endothelial cell proliferation and inflammation is induced via $CysLT_2$/Rho kinase and $CysLT_1$/Erk dependent pathways (44) and indeed quininib is known to inhibit LTD_4 induced phosphorylation of ERK (7). Interestingly, treatment of murine aortic explants with the $CysLT_1$ antagonist montelukast blocks the growth of vascular sprouts, however, antagonism of the $CysLT_2$ using BAY-cyslt2 did not prevent sprouting, suggesting that $CysLT_1$ signaling has a more significant pro-angiogenic role (43). There is also a significant reduction in the incidence of cancer among asthmatic patients treated with the $CysLT_1$ antagonist montelukast (45,46). Given the apparent opposing biological role of these receptors, we demonstrate in this study that our most effective anti-angiogenic analogue Q8 is indeed an antagonist of $CysLT_1$ but not of $CysLT_2$, outlining the potential biological specificity of its effects.

The formation of new blood vessels under developmental and pathological conditions is dependent on the ability of endothelial cells to

migrate beyond the capillary basal lamina following its degradation, proliferate and form capillary tubules with lumens to conduct the flow of blood (47). Here, we show the $CysLT_1$ antagonist Q8 significantly inhibits human endothelial cell proliferation and has the most prominent inhibitory effects on cell migration and tubule formation compared to all other analogues. The effects of Q8 are not associated with significant changes in endothelial cell viability suggesting that the reduction in tubule formation and cell number following Q8 treatment is not due to endothelial cell death. The anti-angiogenic effect of quininib analogues does not depend on the inhibition of endothelial cell proliferation.

Concentrations of 1–10 μM of all analogues tested significantly inhibit tubule formation at 16 hours post treatment compared to control, yet 10 μM of each analogue does not affect cell proliferation in the MTT assay at 24 hours. This data taken together suggests that higher concentrations of analogues may exert their anti-angiogenic effects by causing endothelial cell growth arrest and lower concentrations may inhibit endothelial cell migration but have negligible influence on cell growth.

Pathological angiogenesis is associated with consistent upregulation of many pro-angiogenic mediators including bFGF, Ang-1, Ang-2, VCAM-1, ICAM-1 and VEGF-A. VEGF-A induces endothelial cell proliferation, migration and vessel permeability and is the most recognized driver of cancer related vascular growth and vascular leakage in age-related macular degeneration (48). *In vitro* tubule formation (tubulogenesis), first described in 1980 (49), mimics the fundamental later stage processes of *in vivo* angiogenesis such as endothelial cell adhesion, migration, protease activity and tubule formation (50) and can be significantly enhanced using the native ligand $VEGF\text{-}A_{165}$ (47,48,51). Here, the *in vitro* tubule formation assay applied does not rely on VEGF-A as demonstrated by the ineffectiveness of bevacizumab to significantly reduce total tubule length in the absence of recombinant $VEGF_{165}$. The anti-angiogenic activity of bevacizumab is only apparent in this tubule formation assay following co-administration with recombinant $VEGF_{165}$, a result similarlily exemplified by Han and Papadopoulos (48,51). In this manner, our quinoline compounds do not rely on the presence of VEGF to induce an anti-angiogenic phenotype suggesive of a novel mechanism of action. Furthermore, treatment of human endothelial cells with both quininib analogues and $VEGF_{165}$ reduces the anti-angiogenic activity of the quininib analogues which supports the hypothesis that these novel compounds do not directly inhibit VEGF. The absence of exogenous $VEGF_{165}$ in the combination migration assay (**Fig 2. C**) could explain the lack of effects on endothelial cell migration observed with bevacizumab and consequential lack of significant effects following treatment of cells with a combination of bevacizumab and Q8 compared to Q8 alone (**Fig 2. C**).

The effects of combining anti-angiogenic treatments which have distinct mechanisms of action in cancer models is largely under-investigated (12). We demonstrate for the first time that a combination of the anti-VEGF biological bevacizumab and the novel $CysLT_1$ antagonist Q8 has enhanced additive anti-angiogenic effects *in vitro* compared to treatment with either alone. Jia *et al*, 2007 demonstrated an additive therapeutic effect where pancreatic tumour growth reduction and decreased tumour VEGF expression occurred following treatment of tumour bearing mice with bevacizumab and the Sp1 inhibitor mithramycin A (52). This highlights the importance of this current study concerning the anti-angiogenic additive effects of bevacizumab and Q8 *in vitro*. Moreover, two of the Q8 concentrations (1-3 μM) demonstrating a significant additive inhibitory effect on tubule formation in combination with bevacizumab show no significant inhibition of VEGFR1, VEGFR2 or VEGFR3. This supports a VEGF-independent action of this novel analogue at these concentrations. In cell-based ligand binding assays, inhibition of VEGFR1 with 10 μM Q8 was ~27%, well below the threshold regarded as significant. Also, in human KDR or FLT-4 kinase assays, 1 or 3 μM Q8 inhibited VEGFR2 or VEGFR3 below threshold levels. Interestingly, 10 μM Q8 inhibits VEGFR2 or VEGFR3 above the threshold regarded as significant. This data suggests a dual role for Q8 at higher concentrations wherein the compound may inhibit some VEGF receptors in addition to antagonising $CysLT_1$. However, the relevance of these *in vitro* kinase results to the anti-angiogenic activity in cell lines and in vivo has yet to be determined.

The evidence supporting the pro-angiogenic and pro-tumorigenic role of leukotreine signalling has never been more ostensive (6). We show for the first time that Q8, a novel quinoline antagonist of $CysLT_1$ inhibits pro-vascular phenotypes and also reduces endothelial cell secretions of fundamental pro-angiogenic mediators including VEGF, ICAM-1, VCAM-1, NF-kB and calpain-2. As the activity of the pro-angiogenic cysteine protease calpain-2 is calcium dependent and $CysLT_1$ signalling activates inositol trisphosphate (IP3) (53), we investigated whether the $CysLT_1$ antagonist Q8 would affect levels of this enzyme (54). Calpain-2 is a calcium activated cysteine endopeptidase and a known regulator of VEGF mediated angiogenesis (54). Calpain-2 facilitates IkBα degradation (55), enabling translocation of the VEGF inducer NF-kB to the nucleus. The association between calpain, NF-kB and VEGF expression has been reported (56). In addition, an inhibitor of calpain reduces the levels of phospho-IκBα and inhibits release of pro-inflammatory mediators in mast cells (57). Western blot analysis demonstrates that Q8 significantly reduces calpain-2 levels and this enzyme has been reported to mediate IkBα degradation (55), enabling translocation of the VEGF inducer NF-kB to the nucleus. It is likely that antagonism of $CysLT_1$ by Q8 leads to decreased levels of secreted VEGF through inhibition of NF-kB (30,58). Indeed, in the current study we show that Q8 significantly reduces the activation of the NF-kB p65 unit compared to control. Prevention of angiogenesis through inhibition of NF-kB has long been a focus of anti-cancer therapy and immense efforts have been made to develop specific NF-kB inhibitors (59-61).

The discernible reduction in levels of secreted ICAM-1 and VCAM-1 following treatment of HMEC-1 cells with Q8 may be a result of inhibition of Akt/PKB induced Rho and Rac signalling (17,19) following antagonism of $CysLT_1$. It is well understood that ICAM-1 and VCAM-1 signaling and function is regulated by the Rho-GTPases (18). Leukotriene signaling enhances the expression of ICAM-1 and VCAM-1 (30), where ICAM-1 is known to mediate endothelial progenitor cell (EPC) recruitment (62) and VCAM-1 facilitates endothelial cell-cell interaction (63). VEGF has also been shown to mediate upregulation of endothelial cell VCAM-1 and ICAM-1 through NF-kB activation (64). Q8 reduced secretions of ICAM-1 and VCAM-1 by ~48% and ~44%, respectively, but the parent compound Q1 only reduced the secretions of ICAM-1 and VCAM-1 by ~28% and ~8%, respectively. Analogue Q22 reduced secretions of ICAM-1 and VCAM-1 by ~0% and ~6%, respectively and analogue Q18 reduced secretions of ICAM-1 and VCAM-1 by ~24% and ~9%, respectively. Ang-2 enables vascular de-stabilisation and endothelial activation, enabling access of pro-angiogenic mediators to the endothelium. A reduction in Ang-2 may be the mechanistic output common to all of the quininib series of compounds as Ang-2 was the only angiogenic factor to be significantly down-regulated by all quininib drugs. However, Ang-2 was also downregulated by bevacizumab suggesting that regulation of other factors may be more important for the improved anti-angiogenic effects of the higher ranking quininib analogue Q8. The survival of endothelial cells and the recruitment of pericytes is highly reliant on Ang-1 (65). Q1 and analogues Q8 and Q18 were the only compounds to significantly reduce enothelial cell secretion of Ang-1 by ~66%, ~75% and ~67%, respectively. Q8 reduced endothelial cell secretions of VEGF by ~40%. Q1 and analogue Q22 failed to elicit any changes in secreted VEGF and Q18 reduced VEGF secretion neglibibly by ~4%. The additive anti-angiogenic effects of Q8 in combination with the anti-VEGF bevacizumab may be clarified by the more significant effect of Q8 on levels of ICAM-1 and VCAM-1 in additional to the dual effect of Q8 and bevacizumab on levels of VEGF. A significant up-regulation of bFGF secretion was associated with Q8, possibly due to functional redundancy to compensate for lowered levels of VEGF (64,66).

In conclusion, using an iterative phenotype based ranking approach, we have developed structural analogues of quininib with novel and additive mechanisms of action, most notably analogue Q8, which has the most potent anti-angiogenic activity *in vivo* and *in vitro* compared to all other analogues and is active in VEGF-independent models of angiogenesis. The dual effects of bevacizumab and Q8 on VEGF levels together with the exclusive effects of Q8 on levels of ICAM-1 and VCAM-1 may explain the additive anti-angiogenic effect observed with bevacizumab and Q8 in combination. Such novel small molecules

as the quininib series of compounds offer a novel therapeutic strategy to combat the inefficient clinical efficacy and resistance associated with conventional anti-VEGF therapies.

EXPERIMENTAL PROCEDURES

Ethical Approval. Prior to commencing zebrafish ISV (intersegmental vessel) screens, the study was approved by the UCD Animal Research Ethics Committee under protocol number AREC-P-11-22.

Small molecule chemicals for in vivo and in vitro experiments. 2-[(*E*)-2-(quinolin-2-yl)vinyl]phenol (quininib) analogues were synthesised by Celtic Catalysts (Ireland). Analogues were dissolved in 100% DMSO and diluted in embryo medium to test concentrations of 10-0.1 µM *in vivo* (final DMSO concentration was 0.1%). For *in vitro* experiments, 5-fluorouracil (Sigma F6627), Montelukast (Selleckchem S4211), quininib and its structural analogues, Q22, Q8, and Q18 were dissolved in 100% DMSO as 10 mM stock solutions and stored at -20˚C. Working concentrations (0.1 – 10 µM) were prepared by dissolving stock solution in cell culture media or H_2O giving a final DMSO concentration of 0.1%.

Zebrafish (Danio rerio) Husbandry. Adult transgenic Tg(*fli1*:EGFP) zebrafish which express enhanced green florescent protein (EGFP) in all endothelial cells, were kept on a 14 hr light/10 hr dark cycle at 28˚C. Male and female adult Tg(*fli1*:EGFP) zebrafish were in-crossed to produce embryos which were subsequently staged using morphological assessment to obtain 6 hpf embryos (67).

Intersegmental Vessel Assay. During the primary screen, all compounds were tested at 10µM. During dose dependent screening, the parent compound quininib (Q1) and its analogues Q8, Q18 and Q22 were tested at 0.1-10 µM by incubating with five 6 hpf Tg(*fli1*:EGFP) embryos in 48 well plates for 48 hours. At 2 dpf, the larvae were removed from their chorions and fixed in 4 % paraformaldehyde, left for 2 hours at room temperature, washed with PBS and left at 4˚C before analysed using fluorescent microscopy.

Fluorescent Microscopy. An Olympus SZX16 stereo zoom microscope with an Olympus DP71 camera and cellSens software (Olympus) captured fluorescent and brightfield images of fixed 2 dpf larvae. Intersegmental vessels were manually counted using high magnification and fluorescent images of Tg[*fli1*:EGFP] larvae obtained by EGFP excitation/emission filters (400 nm/509 nm).

Intersegmental vessel assay scoring system for efficacy potency and toxicity. To rank efficacy, compounds which inhibited intersegmental vessel growth in 2 dpf Tg(*fli1*:EGFP) larvae by 80-100% were allocated a score of 5, by 60-79% were allocated a score of 4, by 40-59% were allocated a score of 3, by 20-39% were allocated a score of 2, by 1-19% were allocated a score of 1 and inhibition by 0% scored 0. To rank potency, compounds which could significantly inhibit ISV formation at 0.1 µM were allocated a score of 6, at 0.5 µM scored 5, at 1 µM scored 4, at 2.5 µM scored 3, at 5 µM scored 2 and only at 10 µM scored 1. Potency and efficacy scores contributed to a total ranking score for each compound. Following determination of the lowest concentration of each compound which significantly reduced intersegmental vessel growth, this data was compared to the degree of larval death. Compounds at the lowest effective concentrations which induced larval death by 80-100% were allocated a score of 0, by 60-79% were allocated a score of 1, by 40-59% were allocated a score of 2, by 20-39% were allocated a score of 3, by 1-19% were allocated a score of 4 and if larval death was 0% these compounds scored 5.

Preparation of clinical drugs and recombinant protein for cell based assays. Bevacizumab (Avastin®) (Genentech) (25 mg/ml) was, unless otherwise stated, tested at 2.5 µg/µl. Recombinant $VEGF_{165}$ (R&D Systems cat: 293-VE-010) was reconstituted from lyophilized form to 100 µg/ml using sterile PBS containing 0.1% bovine serum albumin and stored at -20˚C in 10 µl aliquots.

Cell culture. HMEC-1 (human microvascular endothelial cells) were sourced from American Type Culture Collection (ATCC), and maintained at 37˚C / 5% CO_2 in MCDB-131 medium (Gibco/cat: 10372) supplemented with 10% FCS, L-Glutamine (Gibco/cat: 25030-032), 1 µl/ml Hydrocortisone (Sigma/cat: H0396), 10 ng/ml EGF (BD Biosciences 354001) and 1% Pen-Strep (Gibco/cat: 151040-148).

MTT Assay. HMEC-1 cells were trypsinised using 2 ml TrypLE™ Express (1X) (Invitrogen) and centrifuged at 1200 rpm for 4 mins at RT. The cell pellet was resuspended in full media and cells were counted and seeded into 96 well

plates at a density of 10,000 cells/well. Cells were left to adhere for 24 hours and serum starved for 24 hours. Media was removed and replaced with 5, 10 or 20 μM drug. 5-fluorouracil (5-FU) was used as a positive control and DMSO as the vehicle control. HMEC-1 cells were treated with 10 μM analogues only for 24, 72 and 96 hours. Drug solution was removed and wells were washed with PBS before adding 100 μl 100% DMSO to dissolve the formazan crystals. The absorbance values were read at 570 nm using SpectraMax® M2 microplate reader.

Migration Assay. The migration of HMEC-1 human endothelial cells towards a 10% FBS medium solution was observed using a CIM-plate 16 (RTCA DP Analyser, xCelligence Roche). To prepare the CIM-plate, media containing chemoattractant or serum free media was pipetted into each lower well and the upper chamber was clicked into position above these wells. 30 μl serum free media was added to cover the surface of the microporous membrane and the plate was incubated at 37°C in 5% CO_2 for ≥ 1 hour. After this time, a background reading of the plate with no cells was taken. HMEC-1 cells were trypsinised and resuspended in MCDB-131 medium with 10% FBS. 50,000 cells were seeded in duplicate and treated with 10 μM quininib, Q22, Q8, and Q18 analogues or with 0.1% DMSO control. Each CIM-16 plate well has a lower chamber containing 10% FBS as a chemoattractant and an upper chamber containing cells (+/- treatments) in serum free medium. The chambers are separated by a microporous membrane with gold electrodes on the lower side. Cells bind to the gold electrodes when they migrate from the upper chamber through the membrane and cause an electrical impedance which is recorded by an electric sensor plate and which correlates to the number of cells bound. HMEC-1 cells were treated with 2.5 μg/μl bevacizumab and either 1 μM or 3 μM Q8 for combination migration experiments. Cells were left to settle at room temperature for 30 minutes and the CIM-PLATE was placed into the RTCA DP analyser at 37°C in 5% CO_2 and recording of the Cell Index (CI) occurred every 15 minutes. At the 8 hour time point, the CI values were analysed and graphed using the RTCA software (Roche).

In vitro tubule formation assay. The wells of a μ-slide angiogenesis plate (IBIDI) were coated with a layer of matrigel matrix (BD Biosciences) which was left to form a gel for 45 minutes at 37ºC. HMEC-1 cells were grown to 80% confluence, washed with DPBS (Invitrogen) and trypsinised using TrypLE™ Express (1X) (Invitrogen). 7.5 x 10^3 cells were pipetted into each matrigel coated well of the μ-slide angiogenesis plate and treated with either 0.1% DMSO or 1, 3 or 10 μM quininib, and analogues Q22, Q8, Q18, recombinant $VEGF_{165}$ or bevacizumab. The slide was kept at 37ºC/5% CO_2 during tubule formations. Following 16 hours, the cells were imaged by phase contrast microscopy using the Zeiss Axiovert 200 M microscope. Total tubule length (μM) was quantified using Zeiss Axiovision image analysis software.

Calcein AM staining. Calcein AM stain (C3099 Invitrogen) was prepared at 2 μg/ml final concentration and incubated with HMEC-1 cells following tubule formation for 30 minutes at 37ºC. The stain was removed and cells were washed with PBS and serum supplemented cell media was replaced. Cells were visualised and imaged under fluorescent microscopy using the Olympus SZX16 stereo zoom microscope with an Olympus DP71 camera and cellSens software (Olympus).

Cysteinyl leukotriene receptor-1,2 antagonism assay. Q8 was assessed for antagonism of the cysteinyl leukotriene receptor-1 and cysteinyl leukotriene receptor-2 using cell based (CHO and HEK-293) assays (7).

Vascular Endothelial Receptor Assays. For the ligand binding assay, the percentage of bound [^{125}I] VEGF in human recombinant Sf21 cells overexpressing VEGFR1 was quantified by scintillation counting. Evaluation of the inhibitory effects of Q8 on the activity of human KDR kinase (VEGFR2) and human FLT-4 kinase (VEGFR3) were quantified by measuring the phosphorylation of the substrate Ulight-CAGAGAIETDKEYYTVKD (JAK1) using a human recombinant enzyme and the LANCE® detection method (Eurofins Cerep SA). Inhibition higher than 50% is considered significant.

Zebrafish larval $CysLT_1$ expression analysis. RNA was isolated from larvae using Trizol® (Invitrogen) as per manufactures protocol. RNA samples were stored at -80˚C. Concentrations of RNA were obtained using spectrophotometry and quality of samples was deciphered using optical-density (OD) measurements. RNA extracted from larvae was

reversed transcribed to produce cDNA using the SuperScript® III First-Strand Synthesis System for RT-PCR according to the manufacturer's instructions. $CysLT_1$ forward primer [5-GGCATCTTGCGCACTCTACT-3] and $CysLT_1$ reverse primer [5-GCAAAGCGTGATGACCACAG-3] were used to generate PCR products which were electrophoresed for 50 minutes/110V. Gels were visualised with a gel image analysing system (UVP products). Intensities of PCR product bands were normalised to β-actin and sizes verified by loading 5 µl DNA HyperLadder™1 onto the gel.

HMEC-1 $CysLT_1$ and downstream protein expression analysis. HMEC-1 (human dermal derived endothelial cells) were seeded at 250,000 cells per well and following adherence, cells were serum starved for 24 hours. To assess $CysLT_1$ expression, cytosolic and nuclear proteins were extracted from cells using Buffer A (10 mM HEPES pH 8, 1.5 mM $MgCl_2$, 10 mM KCl, 200 mM sucrose, 0.5 mM DTT, 0.25% IGEPAL and 1x protease inhibitor) and Buffer B (20 mM HEPES pH 8, 420 mM NaCl, 0.2 mM EDTA, 1.5 mM $MgCl_2$, 0.5 mM DTT, 25% glycerol and 1x protease inhibitor) respectively. Following treatment of HMEC-1 cells with 10 µM Q1, Q8 or montelukast for 5 hours, total protein was extracted from cells using RIPA lysis buffer supplemented with sodium fluoride (Sigma), β-glycerol-phosphate (Sigma) protease inhibitor (Sigma) and phosphatase inhibitor (Sigma). Protein concentrations were determined using the BCA protein assay kit (Pierce). Expression of proteins of interest were determined by immunoblotting. 20 µg of protein was prepared in 5X sample buffer and separated by 12% SDS/PAGE, transferred to PVDF membranes (Millipore), and probed with primary antibodies ($CysLT_1$: Abcam, [ab151484] 1:2000, Lamin A/C: Cell Signaling [2032] 1:1000, Alpha tubulin: Santa Cruz [sc-32293] 1:200, calpain-2: Aviva Systems Biology [OALA08938] 1:2000, β-actin: Sigma [A5441] 1:5000). Membranes were subsequently probed with anti-rabbit horseradish peroxidase (HRP)-labelled secondary antibody: (Cell Signaling, [7074] 1:2000, or anti-mouse horseradish peroxidase (HRP)-labelled secondary antibody: Cell Signaling [7076] 1:2000). Protein bands were visualized by chemiluminescent detection using Pierce ECL western blotting substrate. Optical densitometry was used to quantitatively measure levels of expressed protein using ImageJ software.

Enzyme Linked Immunosorbent Assays. Following treatment of HMEC-1 cells for 16 hours with 10 µM quininib analogues, secretion of VEGF ICAM-1, VCAM-1, Ang-1, Ang-2 and bFGF were analysed using multi-plex ELISAs (Meso Scale Discovery (MSD) on cell conditioned media according to manufacturer's instructions. Following treatment of HMEC-1 cells for 5 hours with 10 µM quininib analogues, cells lysates were isolated using using RIPA lysis buffer supplemented with sodium fluoride (Sigma), β-glycerol-phosphate (Sigma) protease inhibitor (Sigma) and phosphatase inhibitor (Sigma) and protein concentrations were determined using the BCA protein assay kit (Pierce). 20 µg of cell lysates were analysed for levels of activated NF-kB p65 using a TransAM® NF-kB p65 kit (Active Motif) as per manufacturers instructions.

Statistical analysis. Graphpad Prism version 5 was used for statistical analysis. Differences between group means were determined using a one-way ANOVA with Dunnett's post hoc multiple comparison or Bonferroni's multiple comparison test and student's t-test.

Acknowledgments: We thank Dr. Anne Costello for teaching us the *in vitro* tubule formation assay and providing the HMEC-1 cell line and the Education and Research Centre St. Vincent's University hospital for providing bevacizumab. We thank Dimitri Scholz and Kasia Welzel of the UCD Conway Institute Imaging Core Technology department for assisting with imaging of HMEC-1 tubules. We thank Mr. Kieran Wynne for help with proteomics and Lorraine Burke for assisting with calpain-2 western blot. This work was funded by an Irish Cancer Society scholarship (grant code: CRS13BUT) and by Enterprise Ireland (grant code: CF/20111319).

Conflict of interest: JOS and BNK are inventors on patent US 8916586 B2 and ALR, JOS and BNK are inventors on patent US 9388138 B2.

Author contributions: CTB conducted dose dependent screening of quininib analogues in zebrafish, proliferation, migration, viability, additive and mechanistic experiments in HMEC-1 cells, analysed experimental results, and wrote the paper. ALR carried out initial screening of quininib analogues in the ISV assay and organised commercial assays (Eurofins Cerep SA). MT optimised the endothelial cell migration assay and assisted with analysis of results. ETD and GC assisted with proteomics. BNK devised the project and experiments, assisted with experimental analysis and interpretation of the results and wrote the paper with CTB. JOS assisted with experimental design and analysis and revised and edited the paper.

REFERENCES

1. Timar, J., Dome, B., Fazekas, K., Janovics, A., and Paku, S. (2001) Angiogenesis-dependent diseases and angiogenesis therapy. *Pathology oncology research : POR* **7**, 85-94
2. Riaz, M. K., Bal, S., and Wise-Draper, T. (2016) The impending financial healthcare burden and ethical dilemma of systemic therapy in metastatic cancer. *Journal of surgical oncology*
3. Lambrechts, D., Lenz, H.-J., de Haas, S., Carmeliet, P., and Scherer, S. J. (2013) Markers of Response for the Antiangiogenic Agent Bevacizumab. *Journal of Clinical Oncology* **31**, 1219-1230
4. Administration, F. a. D. (2014) FDA Approval for Bevacizumab. National Cancer Institute
5. Mesange, P., Poindessous, V., Sabbah, M., Escargueil, A. E., de Gramont, A., and Larsen, A. K. (2014) Intrinsic bevacizumab resistance is associated with prolonged activation of autocrine VEGF signaling and hypoxia tolerance in colorectal cancer cells and can be overcome by nintedanib, a small molecule angiokinase inhibitor. *Oncotarget* **5**, 4709-4721
6. Burke, L., Butler, C. T., Murphy, A., Moran, B., Gallagher, W. M., O'Sullivan, J., and Kennedy, B. N. (2016) Evaluation of Cysteinyl Leukotriene Signaling as a Therapeutic Target for Colorectal Cancer. *Frontiers in Cell and Developmental Biology* **4**
7. Reynolds, A. L., Alvarez, Y., Sasore, T., Waghorne, N., Butler, C. T., Kilty, C., Smith, A. J., McVicar, C., Wong, V. H., Galvin, O., Merrigan, S., Osman, J., Grebnev, G., Sjolander, A., Stitt, A. W., and Kennedy, B. N. (2016) Phenotype-Based Discovery of 2-[(E)-2-(Quinolin-2-yl)vinyl]phenol as a Novel Regulator of Ocular Angiogenesis. *The Journal of biological chemistry*
8. Galvin, O., Srivastava, A., Carroll, O., Kulkarni, R., Dykes, S., Vickers, S., Dickinson, K., Reynolds, A., Kilty, C., Redmond, G., Jones, R., Cheetham, S., Pandit, A., and Kennedy, B. N. (2016) A sustained release formulation of novel quininib-hyaluronan microneedles inhibits angiogenesis and retinal vascular permeability in vivo. *Journal of controlled release : official journal of the Controlled Release Society*
9. Murphy, A. G., Casey, R., Maguire, A., Tosetto, M., Butler, C. T., Conroy, E., Reynolds, A. L., Sheahan, K., O'Donoghue, D., Gallagher, W. M., Fennelly, D., Kennedy, B. N., and O'Sullivan, J. (2016) Preclinical validation of the small molecule drug quininib as a novel therapeutic for colorectal cancer. *Sci Rep* **6**, 34523
10. Otrock, Z. K., Mahfouz, R. A. R., Makarem, J. A., and Shamseddine, A. I. (2007) Understanding the biology of angiogenesis: Review of the most important molecular mechanisms. *Blood Cells, Molecules, and Diseases* **39**, 212-220
11. Carmeliet, P. (2003) Angiogenesis in health and disease. *Nature medicine* **9**, 653-660
12. Carmeliet, P. (2005) Angiogenesis in life, disease and medicine. *Nature* **438**, 932-936
13. Organisation, W. H. (2012) GLOBOCAN 2012 - Estimated Cancer Incidence, Mortality and Prevalence Worldwide in 2012. International Agency for Research on Cancer
14. Carmeliet, P., and Jain, R. K. (2000) Angiogenesis in cancer and other diseases. *Nature* **407**, 249-257
15. Carmeliet, P. (2000) Mechanisms of angiogenesis and arteriogenesis. *Nature medicine* **6**, 389-395
16. Papetti, M., and Herman, I. M. (2002) Mechanisms of normal and tumor-derived angiogenesis. *American journal of physiology. Cell physiology* **282**, C947-970
17. van Wetering, S., van den Berk, N., van Buul, J. D., Mul, F. P., Lommerse, I., Mous, R., ten Klooster, J. P., Zwaginga, J. J., and Hordijk, P. L. (2003) VCAM-1-mediated Rac signaling controls endothelial cell-cell contacts and leukocyte transmigration. *American journal of physiology. Cell physiology* **285**, C343-352
18. Cernuda-Morollón, E., and Ridley, A. J. (2006) Rho GTPases and Leukocyte Adhesion Receptor Expression and Function in Endothelial Cells. *Circulation Research* **98**, 757-767
19. Jung, C. H., Lee, W. J., Hwang, J. Y., Seol, S. M., Kim, Y. M., Lee, Y. L., Ahn, J. H., and Park, J. Y. (2012) The role of Rho/Rho-kinase pathway in the expression of ICAM-1 by linoleic acid in human aortic endothelial cells. *Inflammation* **35**, 1041-1048

20. Fojo, T., and Grady, C. (2009) How Much Is Life Worth: Cetuximab, Non–Small Cell Lung Cancer, and the $440 Billion Question. *JNCI Journal of the National Cancer Institute* **101**, 1044-1048
21. Smith , T. J., and Hillner , B. E. (2011) Bending the Cost Curve in Cancer Care. *New England Journal of Medicine* **364**, 2060-2065
22. Bach , P. B. (2009) Limits on Medicare's Ability to Control Rising Spending on Cancer Drugs. *New England Journal of Medicine* **360**, 626-633
23. Montero, A. J., Escobar, M., Lopes, G., Glück, S., and Vogel, C. (2012) Bevacizumab in the Treatment of Metastatic Breast Cancer: Friend or Foe? *Current Oncology Reports* **14**, 1-11
24. Gunther, J. B., and Altaweel, M. M. (2009) Bevacizumab (Avastin) for the Treatment of Ocular Disease. *Survey of Ophthalmology* **54**, 372-400
25. Hurwitz, H., Fehrenbacher, L., Novotny, W., Cartwright, T., Hainsworth, J., Heim, W., Berlin, J., Baron, A., Griffing, S., Holmgren, E., Ferrara, N., Fyfe, G., Rogers, B., Ross, R., and Kabbinavar, F. (2004) Bevacizumab plus irinotecan, fluorouracil, and leucovorin for metastatic colorectal cancer. *N Engl J Med* **350**, 2335-2342
26. Lynch, T. J., Jr., Spigel, D. R., Brahmer, J., Fischbach, N., Garst, J., Jahanzeb, M., Kumar, P., Vidaver, R. M., Wozniak, A. J., Fish, S., Flick, E. D., Leon, L., Hazard, S. J., and Kosty, M. P. (2014) Safety and effectiveness of bevacizumab-containing treatment for non-small-cell lung cancer: final results of the ARIES observational cohort study. *Journal of thoracic oncology : official publication of the International Association for the Study of Lung Cancer* **9**, 1332-1339
27. Loges, S., Schmidt, T., and Carmeliet, P. (2010) Mechanisms of Resistance to Anti-Angiogenic Therapy and Development of Third-Generation Anti-Angiogenic Drug Candidates. *Genes & Cancer* **1**, 12-25
28. Kumler, I., Christiansen, O. G., and Nielsen, D. L. (2014) A systematic review of bevacizumab efficacy in breast cancer. *Cancer treatment reviews* **40**, 960-973
29. Kotz, J. (2012) Phenotypic screening, take two. *Science-Business eXchange*, 1-3
30. Behl, T., Kaur, I., and Kotwani, A. (2016) Role of leukotrienes in diabetic retinopathy. *Prostaglandins & other lipid mediators* **122**, 1-9
31. Kanaoka, Y., Maekawa, A., and Austen, K. F. (2013) Identification of GPR99 protein as a potential third cysteinyl leukotriene receptor with a preference for leukotriene E4 ligand. *The Journal of biological chemistry* **288**, 10967-10972
32. Magnusson, C., Mezhybovska, M., Lorinc, E., Fernebro, E., Nilbert, M., and Sjolander, A. (2010) Low expression of CysLT1R and high expression of CysLT2R mediate good prognosis in colorectal cancer. *European journal of cancer (Oxford, England : 1990)* **46**, 826-835
33. Turtay, M. G., Firat, C., Samdanci, E., Oguzturk, H., Erbatur, S., and Colak, C. (2010) Effects of montelukast on burn wound healing in a rat model. *Clinical and investigative medicine. Medecine clinique et experimentale* **33**, E413-421
34. Kennedy, B. D., Reynolds, A., Kilty, C., O'Sullivan, J., and Baxter, A. D. (2016) Anti-angiogenic compounds. Google Patents
35. Murphy, A., Casey, R., Maguire, A., Tosetto, M., Butler, C., Conroy, E., Sheahan, K., O'Donoghue, D., Gallagher, W., Fennelly, D., Kennedy, B., and O'Sullivan, J. (2016) Preclinical validation of the small molecule drug quininib as a novel therapeutic for colorectal cancer. *Scientific Reports*
36. Tewari , K. S., Sill , M. W., Long , H. J. I., Penson , R. T., Huang , H., Ramondetta , L. M., Landrum , L. M., Oaknin , A., Reid , T. J., Leitao , M. M., Michael , H. E., and Monk , B. J. (2014) Improved Survival with Bevacizumab in Advanced Cervical Cancer. *New England Journal of Medicine* **370**, 734-743
37. Edelman, M. J., and Mao, L. (2013) Resistance to anti-angiogenic agents: a brief review of mechanisms and consequences. *Translational Lung Cancer Research* **2**, 304-307
38. Wang, Z., Dabrosin, C., Yin, X., Fuster, M. M., Arreola, A., Rathmell, W. K., Generali, D., Nagaraju, G. P., El-Rayes, B., Ribatti, D., Chen, Y. C., Honoki, K., Fujii, H., Georgakilas, A. G., Nowsheen, S., Amedei, A., Niccolai, E., Amin, A., Ashraf, S. S., Helferich, B., Yang, X., Guha,

G., Bhakta, D., Ciriolo, M. R., Aquilano, K., Chen, S., Halicka, D., Mohammed, S. I., Azmi, A. S., Bilsland, A., Keith, W. N., and Jensen, L. D. (2015) Broad targeting of angiogenesis for cancer prevention and therapy. *Seminars in Cancer Biology* **35, Supplement**, S224-S243

39. Serbedzija, G. N., Flynn, E., and Willett, C. E. (1999) Zebrafish angiogenesis: a new model for drug screening. *Angiogenesis* **3**, 353-359
40. Savari, S., Vinnakota, K., Zhang, Y., and Sjolander, A. (2014) Cysteinyl leukotrienes and their receptors: bridging inflammation and colorectal cancer. *World journal of gastroenterology : WJG* **20**, 968-977
41. Zamboni, R., Belley, M., Champion, E., Charette, L., DeHaven, R., Frenette, R., Gauthier, J. Y., Jones, T. R., Leger, S., Masson, P., and et al. (1992) Development of a novel series of styrylquinoline compounds as high-affinity leukotriene D4 receptor antagonists: synthetic and structure-activity studies leading to the discovery of (+-)-3-[[[3-[2-(7-chloro-2-quinolinyl)-(E)-ethenyl]phenyl][[3- (dimethylamino)-3-oxopropyl]thio]methyl]thio]propionic acid. *Journal of medicinal chemistry* **35**, 3832-3844
42. Murphy, C. S., Parker, C. J., McCague, R., and Jordan, V. C. (1991) Structure-activity relationships of nonisomerizable derivatives of tamoxifen: importance of hydroxyl group and side chain positioning for biological activity. *Molecular pharmacology* **39**, 421-428
43. Xu, L., Zhang, L., Liu, L., Fang, S., Lu, Y., Wei, E., and Zhang, W. (2010) Involvement of cysteinyl leukotriene receptors in angiogenesis in rat thoracic aortic rings. *Die Pharmazie* **65**, 750-754
44. Duah, E., Adapala, R. K., Al-Azzam, N., Kondeti, V., Gombedza, F., Thodeti, C. K., and Paruchuri, S. (2013) Cysteinyl leukotrienes regulate endothelial cell inflammatory and proliferative signals through CysLT2 and CysLT1 receptors. *Sci. Rep.* **3**
45. Ohd, J. F., Nielsen, C. K., Campbell, J., Landberg, G., Lofberg, H., and Sjolander, A. (2003) Expression of the leukotriene D4 receptor CysLT1, COX-2, and other cell survival factors in colorectal adenocarcinomas. *Gastroenterology* **124**, 57-70
46. Tsai, M.-J., Wu, P.-H., Sheu, C.-C., Hsu, Y.-L., Chang, W.-A., Hung, J.-Y., Yang, C.-J., Yang, Y.-H., Kuo, P.-L., and Huang, M.-S. (2016) Cysteinyl Leukotriene Receptor Antagonists Decrease Cancer Risk in Asthma Patients. *Scientific Reports* **6**, 23979
47. Adair, T. H., and Montani, J.-P. (2010) *Angiogenesis - Angiogenesis Assays*, San Rafael (CA): Morgan & Claypool Life Sciences
48. Papadopoulos, N., Martin, J., Ruan, Q., Rafique, A., Rosconi, M. P., Shi, E., Pyles, E. A., Yancopoulos, G. D., Stahl, N., and Wiegand, S. J. (2012) Binding and neutralization of vascular endothelial growth factor (VEGF) and related ligands by VEGF Trap, ranibizumab and bevacizumab. *Angiogenesis* **15**, 171-185
49. Folkman, J., and Haudenschild, C. (1980) Angiogenesis by capillary endothelial cells in culture. *Transactions of the ophthalmological societies of the United Kingdom* **100**, 346-353
50. Arnaoutova, I., and Kleinman, H. K. (2010) In vitro angiogenesis: endothelial cell tube formation on gelled basement membrane extract. *Nat. Protocols* **5**, 628-635
51. Han, Y. S., Lee, J. E., Jung, J. W., and Lee, J. S. (2009) Inhibitory effects of bevacizumab on angiogenesis and corneal neovascularization. *Graefe's archive for clinical and experimental ophthalmology = Albrecht von Graefes Archiv fur klinische und experimentelle Ophthalmologie* **247**, 541-548
52. Jia, Z., Zhang, J., Wei, D., Wang, L., Yuan, P., Le, X., Li, Q., Yao, J., and Xie, K. (2007) Molecular Basis of the Synergistic Antiangiogenic Activity of Bevacizumab and Mithramycin A. *Cancer research* **67**, 4878-4885
53. Alswied, A., and Parekh, A. B. (2015) Ca2+ Influx through Store-operated Calcium Channels Replenishes the Functional Phosphatidylinositol 4,5-Bisphosphate Pool Used by Cysteinyl Leukotriene Type I Receptors. *The Journal of biological chemistry* **290**, 29555-29566
54. Su, Y., Cui, Z., Li, Z., and Block, E. R. (2006) Calpain-2 regulation of VEGF-mediated angiogenesis. *FASEB journal : official publication of the Federation of American Societies for Experimental Biology* **20**, 1443-1451

55. Schaecher, K., Goust, J.-M., and Banik, N. L. (2004) The Effects of Calpain Inhibition on IkBα Degradation After Activation of PBMCs: Identification of the Calpain Cleavage Sites. *Neurochemical Research* **29**, 1443-1451
56. Spirina, L. V., Kondakova, I. V., Choynzonov, E. L., Chigevskaya, S. Y., Shishkin, D. A., and Kulbakin, D. Y. (2013) Expression of vascular endothelial growth factor and transcription factors HIF-1, NF-kB expression in squamous cell carcinoma of head and neck; association with proteasome and calpain activities. *Journal of cancer research and clinical oncology* **139**, 625-633
57. Lin, T. J. (2009) Inhibition of calpain reduces allergic inflammation. Google Patents
58. Xie, T. X., Xia, Z., Zhang, N., Gong, W., and Huang, S. (2010) Constitutive NF-kappaB activity regulates the expression of VEGF and IL-8 and tumor angiogenesis of human glioblastoma. *Oncology reports* **23**, 725-732
59. Calzado, M. A., Bacher, S., and Schmitz, M. L. (2007) NF-kappaB inhibitors for the treatment of inflammatory diseases and cancer. *Current medicinal chemistry* **14**, 367-376
60. Baud, V., and Karin, M. (2009) Is NF-κB a good target for cancer therapy? Hopes and pitfalls. *Nature reviews. Drug discovery* **8**, 33-40
61. Park, M. H., and Hong, J. T. (2016) Roles of NF-κB in Cancer and Inflammatory Diseases and Their Therapeutic Approaches. *Cells* **5**, 15
62. Wu, Y., Ip, J. E., Huang, J., Zhang, L., Matsushita, K., Liew, C. C., Pratt, R. E., and Dzau, V. J. (2006) Essential role of ICAM-1/CD18 in mediating EPC recruitment, angiogenesis, and repair to the infarcted myocardium. *Circ Res* **99**, 315-322
63. Salajegheh, A. (2016) *Angiogenesis in Health, Disease and Malignancy*, Springer International Publishing Switzerland
64. Lieu, C., Heymach, J., Overman, M., Tran, H., and Kopetz, S. (2011) Beyond VEGF: Inhibition of the Fibroblast Growth Factor Pathway and Antiangiogenesis. *Clinical Cancer Research* **17**, 6130-6139
65. Metheny-Barlow, L. J., and Li, L. Y. (2003) The enigmatic role of angiopoietin-1 in tumor angiogenesis. *Cell Res* **13**, 309-317
66. Lieu, C. H., Tran, H., Jiang, Z. Q., Mao, M., Overman, M. J., Lin, E., Eng, C., Morris, J., Ellis, L., Heymach, J. V., and Kopetz, S. (2013) The association of alternate VEGF ligands with resistance to anti-VEGF therapy in metastatic colorectal cancer. *PloS one* **8**, e77117
67. Tran, T. C., Sneed, B., Haider, J., Blavo, D., White, A., Aiyejorun, T., Baranowski, T. C., Rubinstein, A. L., Doan, T. N., Dingledine, R., and Sandberg, E. M. (2007) Automated, quantitative screening assay for antiangiogenic compounds using transgenic zebrafish. *Cancer research* **67**, 11386-11392

FIGURE LEGENDS

FIGURE 1. Analogues more effectively inhibit developmental angiogenesis compared to quininib *in vivo.* Structural skeleton of the quininib drug series and table listing the differences in chemical structure of all quininib analogues – a synthesis scheme for each chemical is included on patent WO 2014012889 A1 (*A*). Schematic of the intersegmental vessel assay; male and female Tg(*fli1:EGFP*) zebrafish are in-crossed yielding embryos which are treated with quininib analogues at 6 hpf; larvae are dechorionated and fixed at 2dpf and intersegmental vessels are counted by visualising under fluorescent microscopy (*B*). Ranking graph of the bioactivity of 24 salt or amine analogue formulations comparing the ability of 10 μM of each analogue to inhibit developmental angiogenesis in the intersegmental vessel (ISV) assay using Tg[*fli1*:EGFP] zebrafish (*C*). Fluorescent images of Tg[*fli1*:EGFP] treated with most effective concentrations of analogues (0.1% DMSO, 10 μM sunitinib, 10 μM Q1, 10 μM Q22, 1 μM Q8 and 5 μM Q18) (*D*). Dose response graph following re-screening of quininib analogues in the ISV assay at concentrations increasing from 0.1-10 μM (*E*). Individual experiments consisted of treating 5 embryos per well in duplicate (10 embryos) and individual experiments were conducted three times (N=3). Statistical analysis was performed by ANOVA and Dunnett's or Bonferroni's post hoc multiple comparison test. Error bars are mean ± SEM. *p<0.05, **p<0.01, ***p<0.001.

TABLE 1. Analogue ISV dose response and ranking of quininib analogues based on efficacy, potency and toxicity

FIGURE 2. Quininib analogues reduce endothelial cell number after 24 hours and inhibit endothelial cell migration. Effect of 10 μM quininib analogues on HMEC-1 endothelial cell number using the MTT assay following 24, 72 and 96 hours treatment; 10,000 cells were seeded and treated in duplicate for each individual experiment and individual experiments were conducted three times (N=3) (*A*). Effect of 10 μM quininib analogues on HMEC-1 endothelial cell migration; 50,000 cells were seeded and treated in duplicate for each individual experiment and individual experiments were conducted three times (N=3) (*B*). Effect of Q8 in combination with bevacizumab on HMEC-1 endothelial cell migration; 50,000 cells were seeded and treated in duplicate for each individual experiment and individual experiments were conducted three times (N=3) (*C*). Migration was assessed using the xCELLigence system (Roche) and RTCA software allowing real time monitoring of cell migration over 8 hours; The real-time traces represent averaged data of all detected/bound cells at one time point (8 hours) (*C*). Statistical analysis was performed by ANOVA and Dunnett's post hoc multiple comparison test and student's t-test. Error bars are mean ± SEM. *p<0.05, **p<0.01, ***p<0.001

FIGURE 3. Quininib analogues inhibit human endothelial cell tubule formation and do not affect HMEC-1 viability. Total tubule length following tubule formation of HMEC-1 endothelial cells treated with 1, 3 or 10 μM quininib analogues for 16 hours; 7,500 cells were seeded in μ-slide angiogenesis wells (IBIDI) and treated in duplicate for each individual experiment and individual experiments were conducted six times (N=6) (*A*). Representative tubule images following treatment of HMEC-1 endothelial cells with 10 μM quininib (Q1) or analogues Q8, Q18 and Q22 for 16 hours (*B*). Viability images of Q8 (0.1-20 μM) treated HMEC-1 endothelial cell tubules stained with calcein AM and propidium iodide; 7,500 cells were seeded in μ-slide angiogenesis wells (IBIDI) and treated in duplicate for each individual experiment and individual experiments were conducted three times (N=3) (*C*). Statistical analysis was performed by ANOVA and Dunnett's post hoc multiple comparison test. Error bars are mean ± SEM. *p<0.05, **p<0.01, ***p<0.001.

FIGURE 4. Quininib analogues inhibit VEGF-independent angiogenesis *in vitro.* HMEC-1 endothelial cell tubule formation is not affected following 16 hour treatment with bevacizumab alone, however, when cells are treated with a combination of recombinant VEGF and bevacizumab, a significant reduction in tubule formation occurs following 16 hours; 7,500 cells were seeded in μ-slide angiogenesis wells (IBIDI) and treated in duplicate for each individual experiment and individual experiments were conducted three

times (N=3) (*A*). Representative tubule images of HMEC-1 cells treated with bevacizumab alone or in combination with recombinant VEGF (*B*). The effects of quininib (Q1) and analogue Q8 on HMEC-1 tubule formation are significantly diminished when cells are treated in combination with VEGF; 7,500 cells were seeded in µ-slide angiogenesis wells (IBIDI) and treated in duplicate for each individual experiment and individual experiments were conducted three times (N=3) (*C*). Tubule images of HMEC-1 cells treated with quininib (Q1) or analogue Q8 alone or in combination with VEGF (*D*). Statistical analysis was performed by ANOVA and Dunnett's or Bonferroni's post hoc multiple comparison test and student's t-test. Error bars are mean ± SEM. *p<0.05, **p<0.01, ***p<0.001

FIGURE 5. Q8 has additive anti-angiogenic effects with an anti-VEGF biologic, bevacizumab. HMEC-1 endothelial cell tubule formation was significantly reduced following 16 hour treatment with analogue Q8 in combination with bevacizumab compared to treatment with Q8 or bevacizumab alone. Quininib (Q1) did not significantly reduce tubule formation in combination with bevacizumab compared to treatment with quininib or bevacizumab alone; 7,500 cells were seeded in µ-slide angiogenesis wells (IBIDI) and treated in duplicate for each individual experiment and individual experiments were conducted three times (N=3) (*A*). Representative tubule images of HMEC-1 endothelial cells treated with analogue Q8 or quininib (Q1) alone or in combination with bevacizumab for 16 hours (*B*). Statistical analysis was performed by ANOVA and Dunnett's or Bonferroni's post hoc multiple comparison test and student's t-test. Error bars are mean ± SEM. *p<0.05, **p<0.01, ***p<0.001

FIGURE 6. Quininib analogue Q8 is a cysteinyl leukotriene receptor-1 antagonist which affects inflammatory and angiogenic signalling pathways. The $CysLT_1$ receptor IC_{50} of analogue Q8 was determined to be 4.9 µM following testing in a cell-based $CysLT_1$ receptor antagonist assay in CHO cells (Eurofins Cerep SA). The assay measured calcium mobilisation using fluor-3-loaded CHO cells overexpressing $CysLT_1$ and stimulated with the $CysL_1TR$ agonist LTD_4. 20 µM Q8 inhibited $CysLT_1$ activation by 105.4%. In contrast, 30 µM Q8 produced only a 22.9% antagonism of $CysLT_2$ receptor activation in HEK-293 cells. Thus, Q8 was excluded as a tangible $CysLT_2$ antagonist as results showing an inhibition lower than 50% were not considered significant; treatment of cells for individual experiments were carried out in duplicate and each experiment was condicted 3 times (N=3). (*A*). $CysLT_1$ is present in our angiogenesis models shown by presence of the $CysLT_1$ transcript in zebrafish larvae at 6 hpf, 1 *dpf, 2 dpf and 3 dpf following PCR and presence of the nuclear form of the receptor in HMEC-1 endothelial cells by western blot; PCR was carried out using RNA isolated from larvae during three separate experiments (N=3) and western blots were conducted three separate times using protein lysates from cells treated in duplicate during three separate experiments (N=3) (*B*)**.** Western blot of HMEC-1 cells treated for 5 hours with 0.1% DMSO or 10 µM Q1, Q8 and montelukast. Expression of calpain-2, a putative calcium sensitive downstream target of $CysLT_1$ signalling and pro-angiogenic mediator is reduced following treatment of endothelial cells with 10 µM Q8; the calpain-2 western blot was conducted on protein lysates from cells treated during three separate experiments (N=3) (*C*). The levels of activated NF-kB p65 were significantly reduced following treatment of HMEC-1 cells with 10 µM Q8 for 5 hours, whereas treatment of cells with 10 µM Q1 or the clinically used $CysLT_1$ antagonist Montelukast for 5 hours had no effect on levels of activated NF-kB p65; NF-kB p65 ELISA was conducted using protein isolated from cells treated on three separate occasions in duplicate (N=3) (*D*). ELISA of HMEC-1 endothelial cell conditioned media following 16 hour treatment of cells with 10 µM quininib (Q1), Q8, Q22 and Q18 revealing significant reductions in important pro-angiogenic mediators angiopoietin-2, VEGF, ICAM-1 and VCAM-1. Compared to other analogues of quininib (Q1), Q8, our highest ranking analogue, was the only compound to significantly reduce soluble ICAM, VCAM and VEGF; conditioned media collected from three separate experiments was analysed in duplicate by ELISA (N=3) (*E*). 10 µM Q8 does not inhibit VEGFR1 and 10 µM Q8 inhibits VEGFR2 and VEGFR3 by 65% and 75% respectively. However, 1-3 µM Q8 does not significantly inhibit VEGFR2 and VEGFR3 where 1 and 3 µM Q8 inhibited VEGFR2 by -34% and -25% respectively and 1 and 3 µM Q8 inhibited VEGFR3 by 29% and 46% respectively. Results showing an inhibition higher than 50% are considered to represent significant effects of the test compounds; experiments were carried

out using duplicate samples during one experiment (Eurofins Cerep SA) (N=1) (*F*). *dpf = days post fertilization. Statistical analysis was performed by ANOVA and Dunnett's post hoc multiple comparison test and student's t-test. Error bars are mean ± SEM. *p<0.05, **p<0.01, ***p<0.001.

FIGURE 7. Proposed effects of combined targeting of $CysLT_1$ and VEGFR2 during angiogenesis. Signalling schematic of $CysLT_1$ and VEGFR2; following antagonism of $CysLT_1$, Q8 inhibits many of the instrumental processes which regulate angiogenesis such as cell motility, cytoskeletal reorganization, proliferation and survival. Ca^{2+} influxes following Q8 antagonism are prevented and the calcium activated cysteine endopeptidase, calpain-2, can no longer facilitate IkBα degradation. Hence, NF-kB is stabilised and will not translocate to the nucleus to induce expression of the angiogenic mediator, VEGF. Additionally, antagonism of $CysLT_1$ by Q8, as demonstrated by ELISA, decreases the expression of ICAM-1 and VCAM-1, preventing endothelial cell motility and endothelial cell precursor recruitment. The enhanced additive anti-angiogenic activity of Q8 is likely due to dual downregulation of VEGF by Q8 and bevacizumab and the exclusive effects of Q8 on secreted levels of ICAM-1 and VCAM-1 (*A*).

A. Structures of quininib analogues

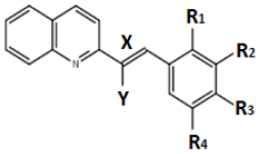

Compound	IUPAC name	X	Y	R_1	R_2	R_3	R_4	Salt
Q1-Quininib	2-[(*E*)-2-Quinolin-2-yl)vinyl]phenol	Alkene	-	OH	-	-	-	-
Q2	2-[(*E*)-2-Quinolin-2-yl)vinyl]phenol HCl salt	Alkene	-	OH	-	-	-	HCl
Q3	3-(2-Quinolin-2-yl-vinyl)-phenol	Alkene	-	-	OH	-	-	-
Q4	3-(2-Quinolin-2-yl-vinyl)-phenol HCl salt	Alkene	-	-	OH	-	-	HCl
Q5	4-(2-Quinolin-2-yl-vinyl)-phenol	Alkene	-	-	-	OH	-	-
Q6	4-(2-Quinolin-2-yl-vinyl)-phenol HCl salt	Alkene	-	-	-	OH	-	HCl
Q7	(E)-2-(2-Quinolin-2-yl-vinyl)- -benzene-1,4-diol	Alkene	-	OH	-	-	OH	-
Q8	(E)-2-(2-Quinolin-2-yl-vinyl)- -benzene-1,4-diol HCl salt	Alkene	-	OH	-	-	OH	HCl
Q9	(E)-2-(2-Quinolin-2-yl-vinyl)- -benzene-2,4-diol	Alkene	-	-	OH	-	OH	-
Q10	(E)-2-(2-Quinolin-2-yl-vinyl)-benzene-2,4-diol HCl salt	Alkene	-	-	OH	-	OH	HCl
Q11	2-(2-Quinolin-2-yl-ethyl)-phenol	Alkane	-	OH	-	-		-
Q12	2-(2-Quinolin-2-yl-ethyl)-phenol HCl salt	Alkane	-	OH	-	-	-	HCl
Q13	3-(2-Quinolin-2-yl-ethyl)-phenol	Alkane	-	-	OH	-	-	-
Q14	3-(2-Quinolin-2-yl-ethyl)-phenol HCl salt	Alkane	-	-	OH	-	-	HCl
Q15	4-(2-Quinolin-2-yl-ethyl)-phenol	Alkane	-	-	-	OH	-	-
Q16	4-(2-Quinolin-2-yl-ethyl)-phenol HCl salt	Alkane	-	-	-	OH	-	HCl
Q17	(Z)-2-(2-(Quinolin-2-yl)vinyl) phenol	Z-Alkene	-	OH	-	-	-	-
Q18	(Z)-2-(2-(Quinolin-2-yl)vinyl) phenol HCl salt	Z-Alkene	-	OH	-	-	-	HCl
Q19	(E)-2-(2-Quinolin-2-yl-propenyl)-phenol	Alkene	Me	OH	-	-	-	-
Q20	(E)-2-(2-Quinolin-2-yl-propenyl)-phenol HCl salt	Alkene	Me	OH	-	-	-	HCl
Q21	2-Quinolin-2-yl-ylethynyl-phenol	Alkyne	-	OH	-	-	-	-
Q22	2-Quinolin-2-yl-ylethynyl-phenol HCl salt	Alkyne	-	OH	-	-	-	HCl
Q23	3-Quinolin-2-yl-ylethynyl-phenol	Alkyne	-	-	OH	-	-	-
Q24	3-Quinolin-2-yl-ylethynyl-phenol HCl salt	Alkyne	-	-	OH	-	-	HCl
Q25	4-Quinolin-2-yl-ylethynyl-phenol	Alkyne	-	-	-	OH	-	-
Q26	4-Quinolin-2-yl-ylethynyl-phenol HCl salt	Alkyne	-	-	-	OH	-	HCl

B. ISV assay

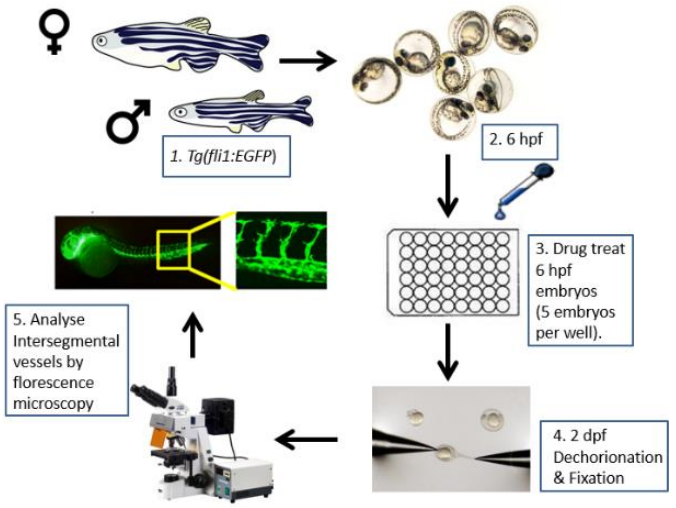

C. ISV screening of quininib analogues

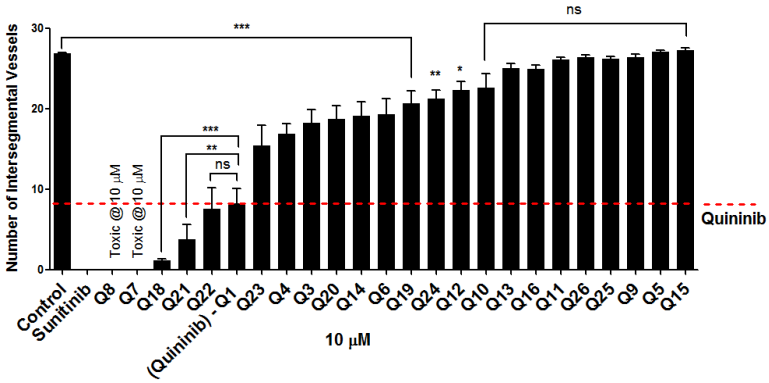

D. ISV images - analogue treated larvae (2dpf)

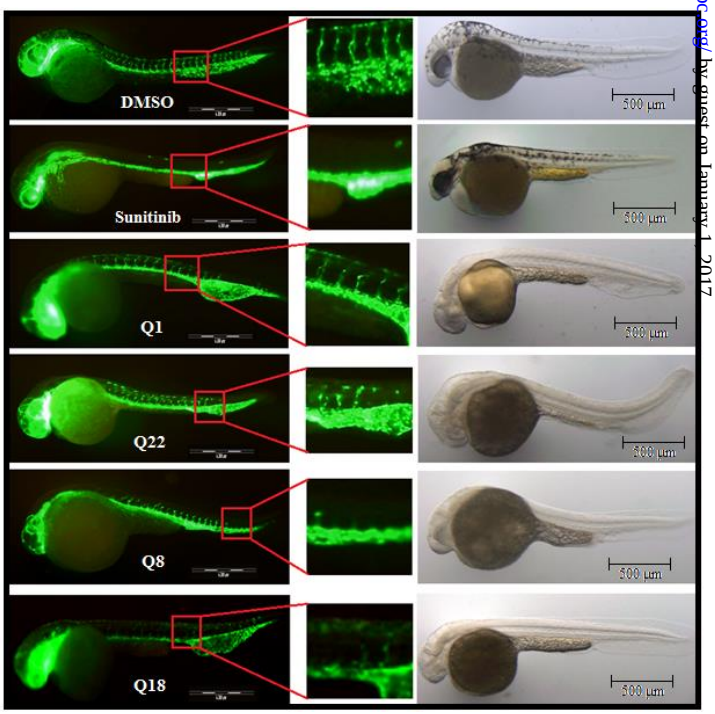

E. ISV dose response highest ranking analogue salts

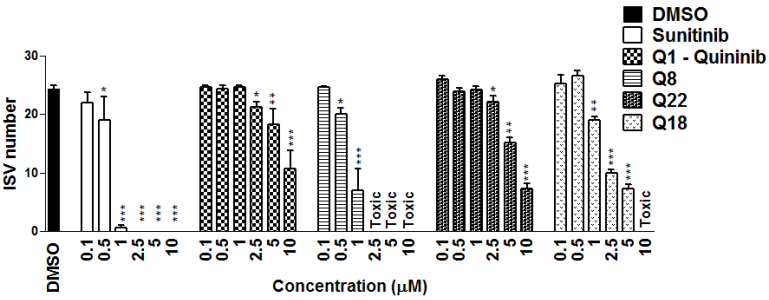

Figure 1. Analogues more effectively inhibit developmental angiogenesis compared to quininib *in vivo*

A. MTT Assay HMEC-1 cells

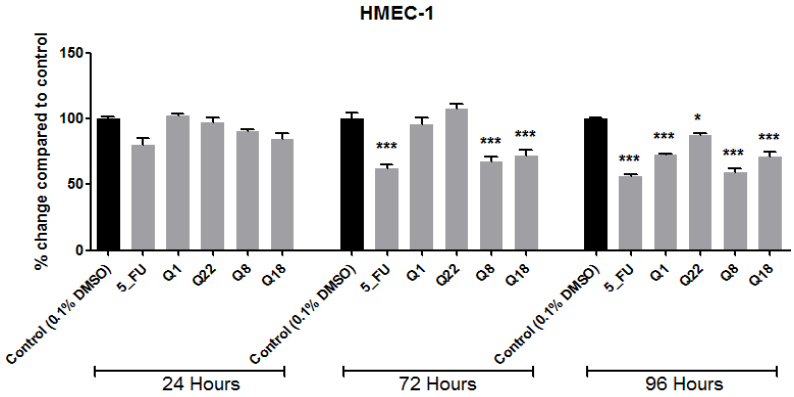

B. HMEC-1 migration over 8 hours and real time migration chart

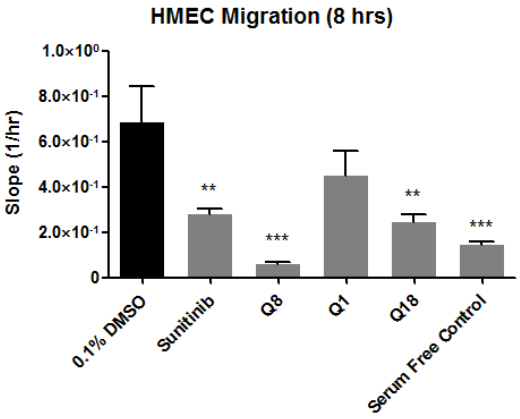

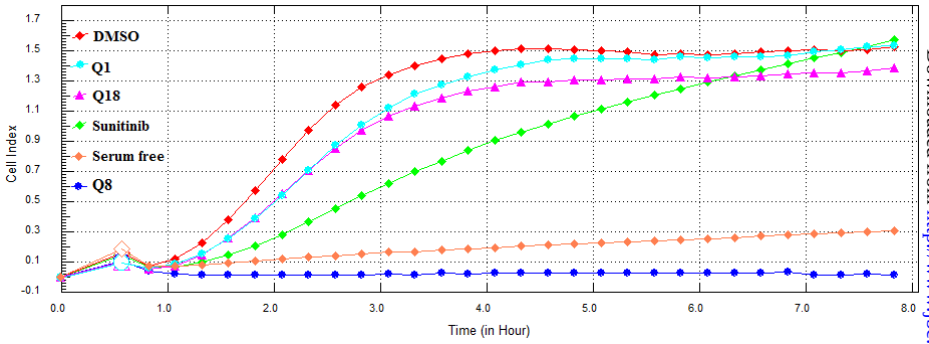

C. HMEC-1 combination migration over 8 hours and real time migration chart

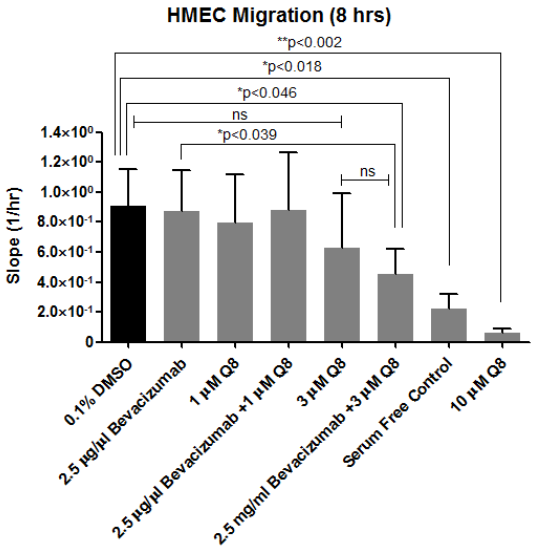

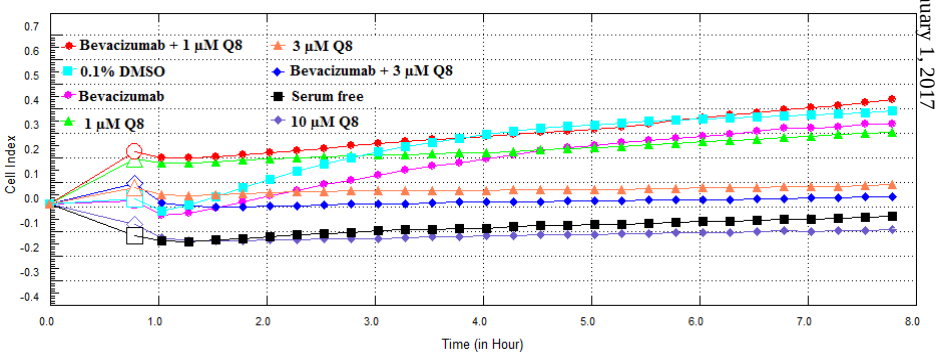

Figure 2. Quininib analogues reduce endothelial cell number after 24 hours and inhibit endothelial cell migration.

A. HMEC-1 tubule formation –analogue dose response

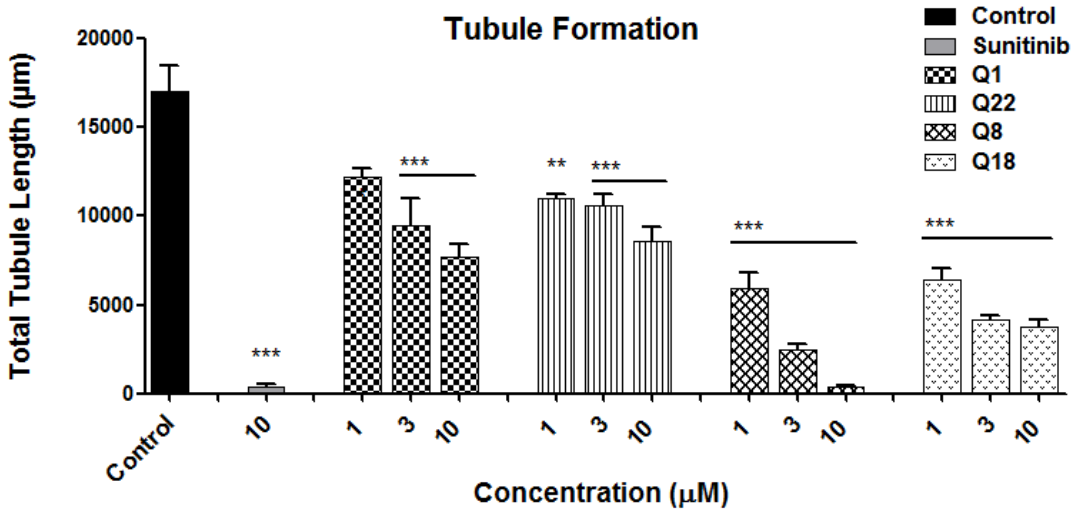

B. Tubule images of analogue treated HMEC-1 cells

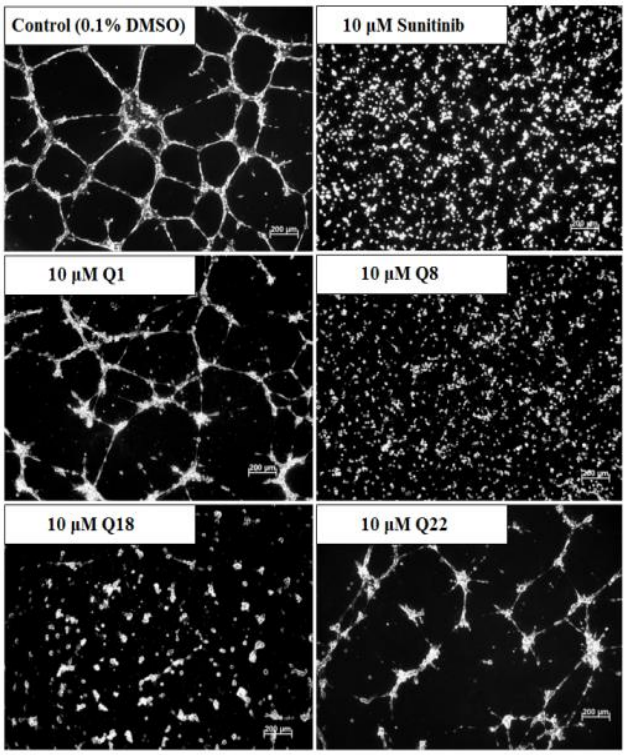

C. Q8 treated HMEC-1 viability (Calcein AM/Propidium Iodide)

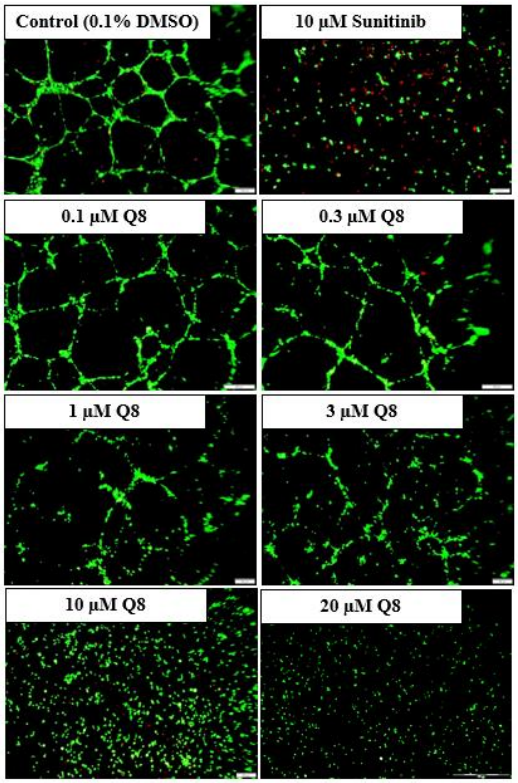

Figure 3. Quininib analogues inhibit human endothelial cell tubule formation and do not affect HMEC-1 viability.

A. Tubule formation – Bevacizumab + $VEGF_{165}$

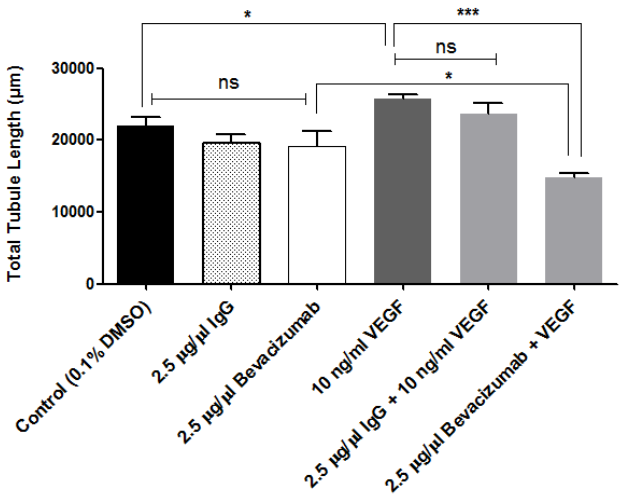

B. Tubule images - Bevacizumab + $VEGF_{165}$

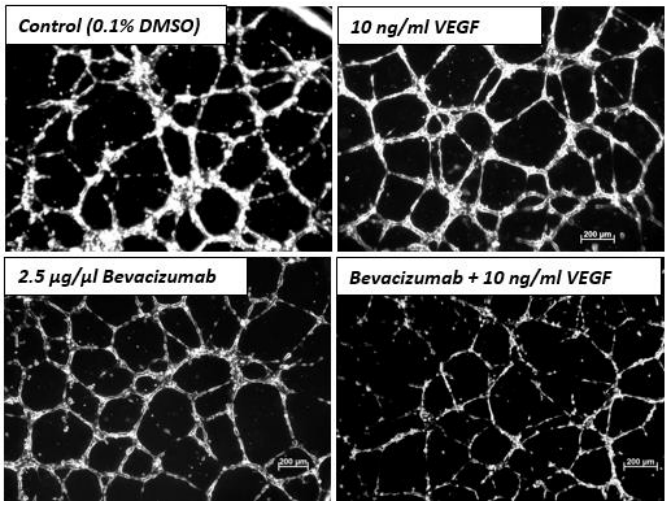

C. Tubule formation – analogues + $VEGF_{165}$ $VEGF_{165}$

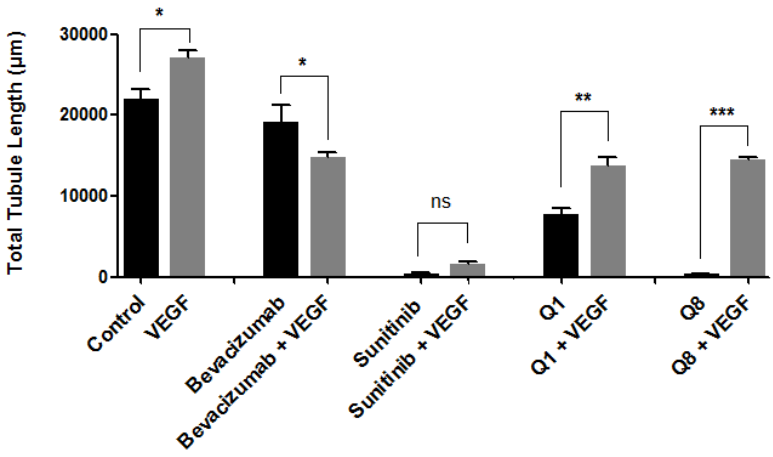

D. Tubule formation images - analogues + $VEGF_{165}$

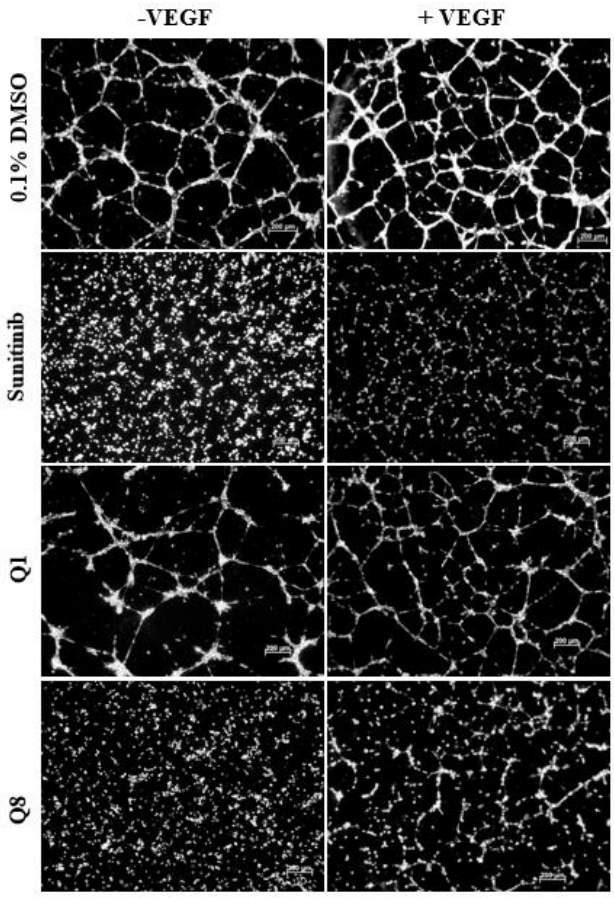

Figure 4. Quininib analogues inhibit VEGF-independent angiogenesis *in vitro*.

A. Tubule formation – Q8 or Q1 + $VEGF_{165}$ + bevacizumab

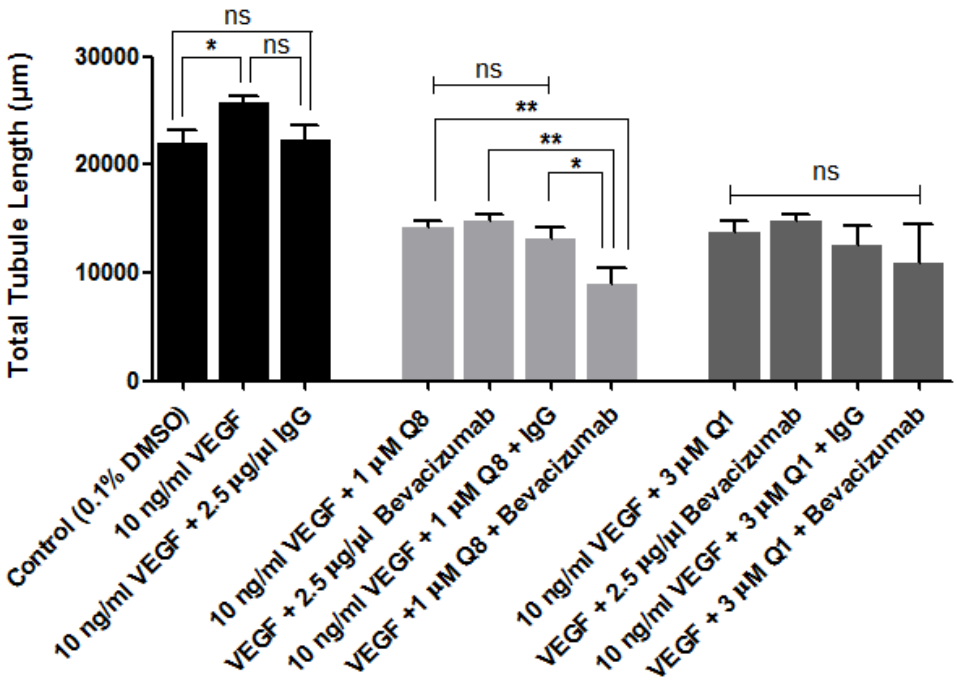

B. Tubule formation – analogues + $VEGF_{165}$ + bevacizumab

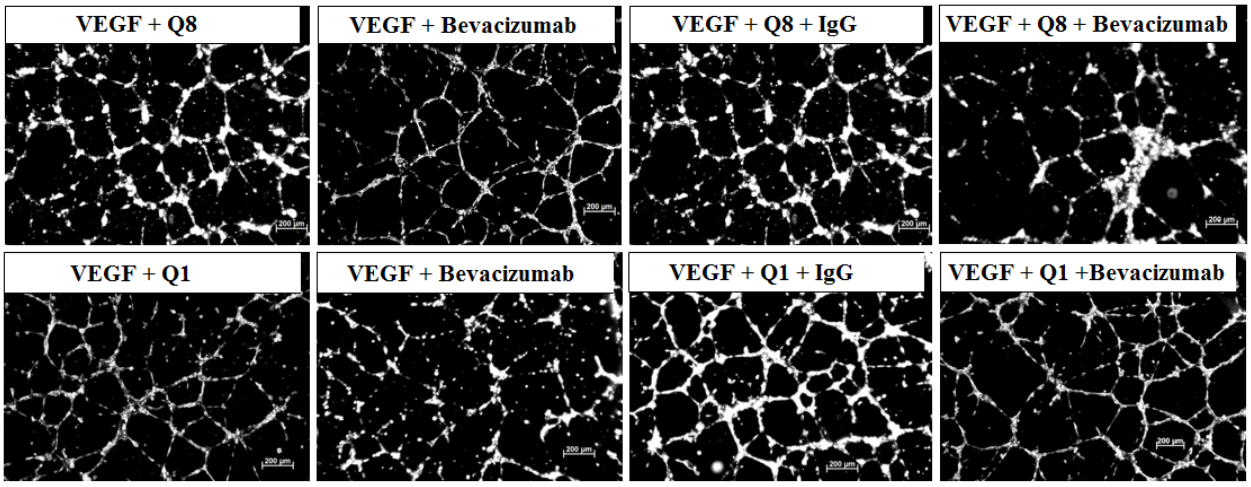

Figure 5. Q8 has additive anti-angiogenic effects with an anti-VEGF biologic, bevacizumab.

A. Q8 IC_{50} of $CysLT_1$

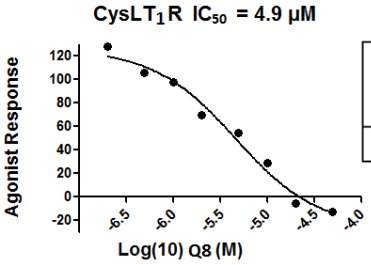

% inhibition $CysLT_1R$ (20 µM Q8)	% inhibition $CysLT_2R$ (30 µM Q8)
105.4	22.9

B. Expression of $CysLT_1$ in zebrafish larvae and HMEC-1 cells

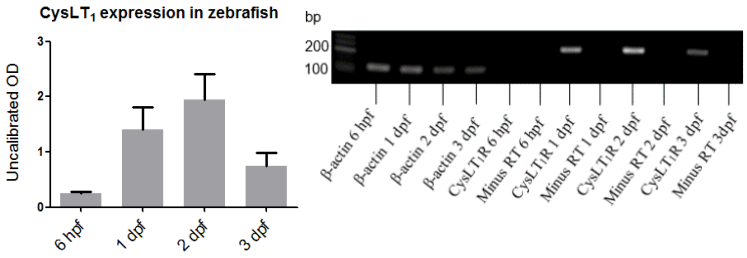

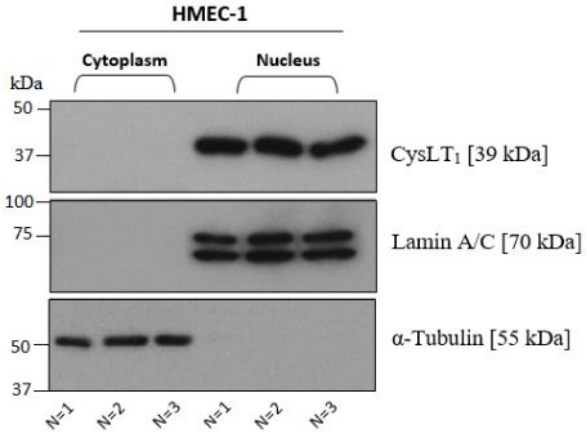

C. Analogue effect on calpain-2 expression

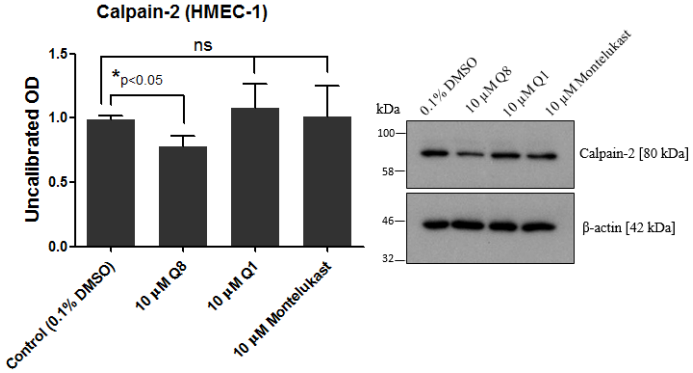

D. Analogue effect on NF-kB activation

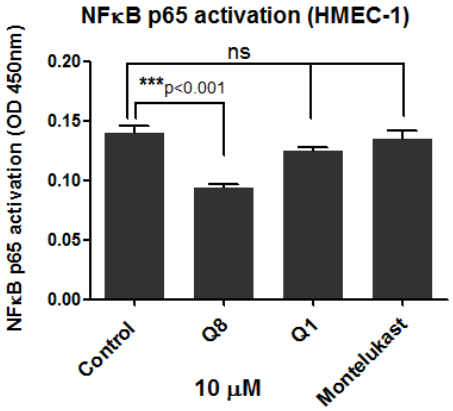

E. HMEC-1 ELISA

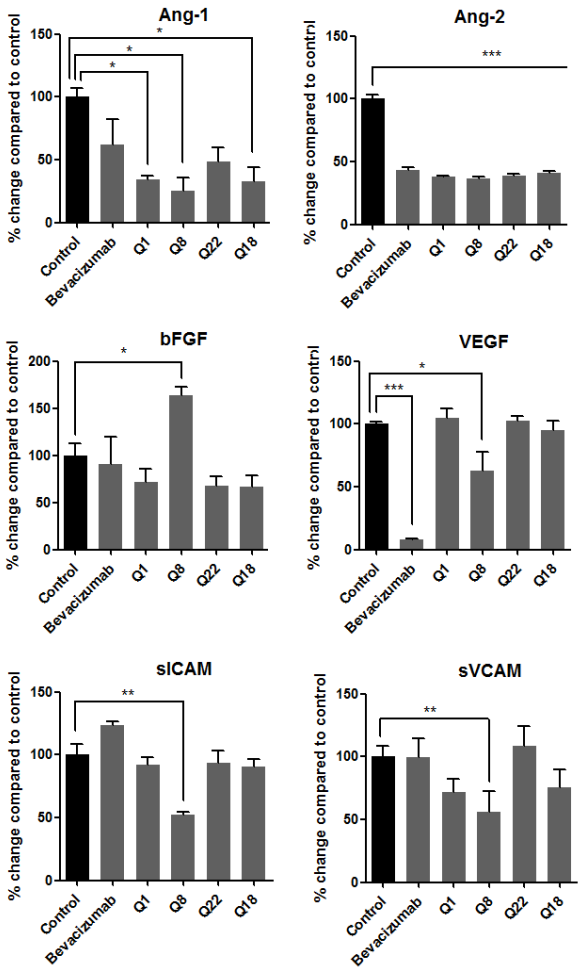

Figure 6. Quininib analogue Q8 is a cysteinyl leukotriene receptor-1 antagonist which affects inflammatory and angiogenic signalling pathways.

A.

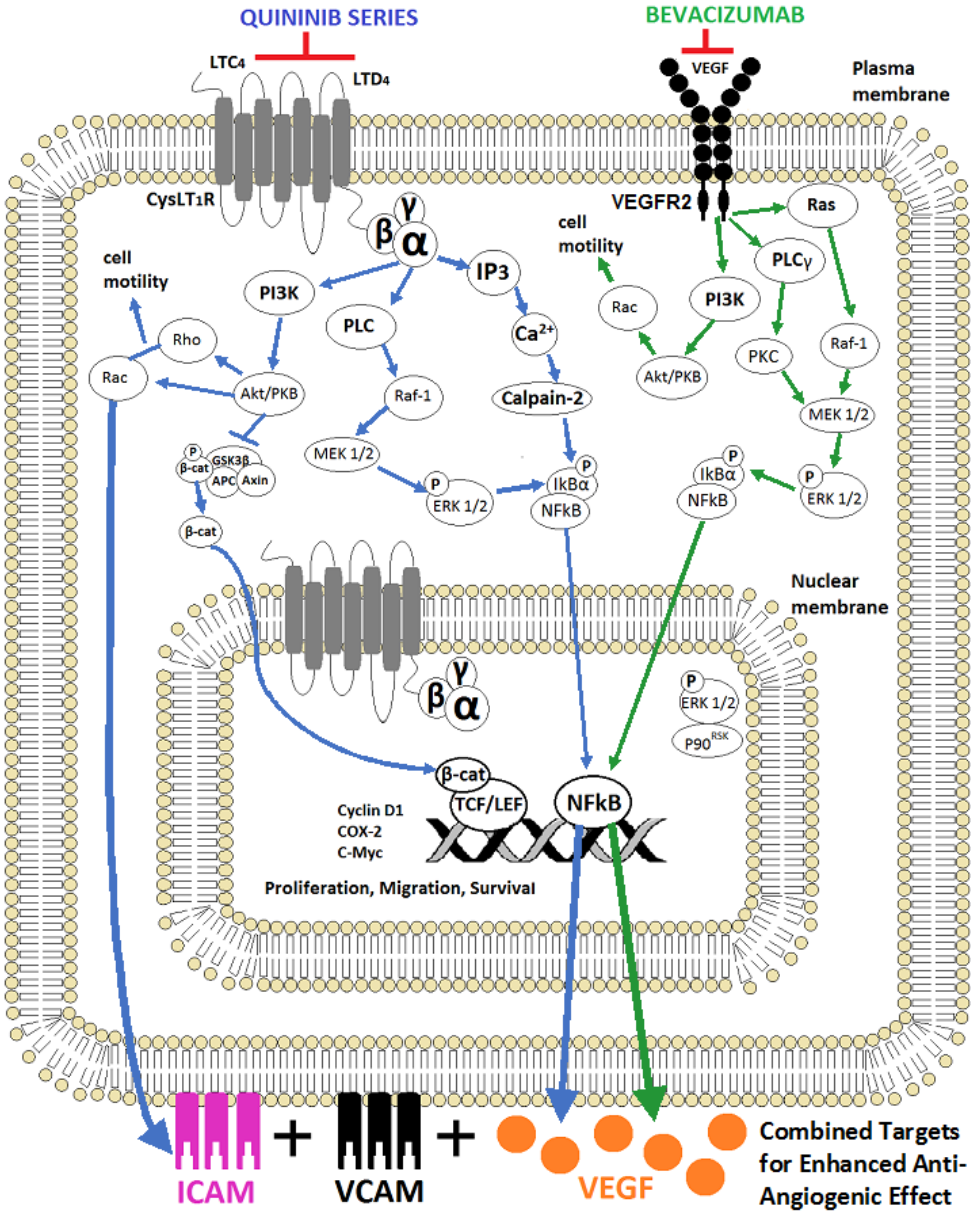

Drug	Pathway	ICAM % reduction	VCAM % reduction	VEGF % reduction
Q8	cysLT antagonist	48	44	37
Bevacizumab	VEGF antagonist	0	0	92

Figure 7. Proposed effects of combined targeting of $CysLT_1$ and VEGFR2 during angiogenesis.

A Quininib Analogue and Cysteinyl Leukotreine Receptor Antagonist inhibits VEGF-Independent Angiogenesis and Exerts an Additive Anti-angiogenic Response with Bevacizumab

Clare T Butler, Alison L Reynolds, Miriam Tosetto, Eugene T Dillon, Patrick Guiry, Gerard Cagney, Jacintha O'Sullivan and Breand&aacuten N Kennedy

J. Biol. Chem. published online December 29, 2016
